Received: 11 February 2025 | Revised: 29 April 2025 | Accepted: 2 June 2025

DOI: 10.1111/joa.70007

Journal of Anatomy ANATOMICAL SOCIETY WILEY

ORIGINAL ARTICLE

Osteology and arthrology of the ankle and tarsometatarsus of anoles (Iguania: Anolidae): not convergent with geckos but divergent from the ancestral iguanian condition

Anthony P. Russell[1] | Lisa D. McGregor[1] | Timothy E. Higham[2]

[1]Department of Biological Sciences, University of Calgary, Calgary, Alberta, Canada

[2]Department of Evolution, Ecology, and Organismal Biology, University of California, Riverside, California, USA

Correspondence
Anthony P. Russell, Department of Biological Sciences, University of Calgary, 2500 University Drive NW, Calgary, AB, Canada T2N 1N4.
Email: arussell@ucalgary.ca

Funding information
Natural Sciences and Engineering Research Council of Canada, Grant/Award Number: A9745-2008

Abstract

The ankle joint of lizards has a complex structure, and its features help to define the Lacertilia. The configuration of this joint in its ancestral state entrains conjoint flexion-extension and long-axis rotation of the pes relative to the long axis of the crus. In *Gekko gecko* these actions can be decoupled because of derived features of the ankle joint. The increased degrees of freedom of the motions of the pes are associated with the operation of the adhesive toe pads carried on the digits. Among iguanian lizards, the genus *Anolis* has independently acquired a digital adhesive system that employs toe pads. Geckos and anoles are thus regarded as being convergent in the possession of a digital adhesive apparatus. This raises the question of whether anoles exhibit a similar ankle structure to that of geckos to allow them to deploy their toe pads in a mechanically similar fashion. Comparative analysis reveals that this is not the case, and that *Anolis* retains an ankle structure very similar to that of its iguanian relatives and non-gekkotan lizards in general. Some differences set its ankle and foot structure apart from those of its closest relatives, but these exaggerate the differences between geckos and anoles rather than lessen them: its ankle joint architecture is more sharply contoured than that of its close iguanian relatives; the ventral peg on the fourth distal tarsal is more extensive; its metatarsals are more gracile in form, relatively longer, and their distal joints are all unicondylar; its fifth metatarsal has a longer shaft and a less prominently sculpted ventral surface; and the meniscus that intervenes between the anterodistal extremity of the astragalocalcaneum and the more medial of the metatarsals is more extensive. These attributes combine to limit degrees of freedom at the ankle joint but provide the digits with greater mobility relative to the metatarsals. Such derived features may prove to be associated with enhanced capabilities for grasping narrow perches, sprinting and jumping, activities common to anoles but much less evident for geckos. The ways in which geckos and anoles negotiate their locomotor environments may be associated with the differences evident in their ankle and tarsometatarsus structure—anoles seemingly using the combination of their toe pads and claws to navigate along and

between relatively narrow branches and geckos using broader, more expansive sectors of the substratum. Anoles and geckos have incorporated adhesive toe pads into their locomotor apparatus from structurally different starting points, with the former integrating the adhesive system into a pedal configuration that departs little from the ancestral lacertilian pattern. Beyond the possession of toe pads the pedal structure of anoles exhibits little in the way of convergence with that of geckos.

KEYWORDS
adhesive system, arthrology, ecomechanics, ligaments, lizards, osteology

1 | INTRODUCTION

The lacertilian ankle joint has a complex geometry (Brinkman, 1980; Higham et al., 2021; Rewcastle, 1980; Russell, 1993; Russell & Bauer, 2008), and is probably the most intricately configured of lizard diarthrotic articulations. It is stabilized by the reciprocal contours of its constituent elements as well as by the ligaments that bind them (Russell, 1993). The continuity of muscles and their associated aponeuroses across the ankle joint, from the crus to the pes, furnish the basis for dynamic and continuously adjustable control (Russell, 1993) and the associated ligaments provide passive governance (Rewcastle, 1980).

Features of the lacertilian ankle and pes contribute a suite of synapomorphic attributes that help define the clade: a fused astragalocalcaneum; an enlarged fourth distal tarsal; and a mediolaterally hooked and dorsoventrally inflected fifth metatarsal (Borsuk-Białynicka, 2018; Evans, 2003). The complex morphology of the fifth metatarsal enables the fifth pedal digit to diverge from, and operate somewhat independently of, the other four digits and serves as a major site of insertion for muscles that drive pedal plantarflexion (Evans, 2003; Robinson, 1975).

In non-gekkotan lizards, the mesotarsal ankle joint entrains conjoint long axis rotation and flexion/extension of the pes through the form of its reciprocally occluding, self-guiding facets (Rewcastle, 1980). Recently, Higham et al. (2021) described derived features of the ankle joint of the gekkotan *Gekko gecko* (Linnaeus, 1758), noting that, compared to lizards in general (Brinkman, 1980; Rewcastle, 1980; Russell & Bauer, 2008), it is configured to permit segregation of pedal flexion/extension and long axis rotation. Geckos are well-known for their effective and morphologically complex adhesive toe pads (Figure 1a,c) (Russell, 1975, 2002; Russell & Gamble, 2019). Deployment of these in static clinging (Russell & Oetelaar, 2016) and dynamic, adhesively assisted locomotion (Birn-Jeffery & Higham, 2014; Russell & Higham, 2009; Song et al., 2020) is associated with a wide range of abduction/adduction of the pes relative to the long axis of the crus that may facultatively be divorced from pedal long axis rotation (Higham et al., 2021). Such versatility of pedal displacement may be associated with the presence and operation of the gekkotan adhesive system (Higham et al., 2021) or may be related to other, as yet unidentified, more general aspects of gecko locomotion in association with the secondarily symmetrical pes of these lizards (Russell et al., 1997).

When compared to *Iguana iguana* (Linnaeus, 1758) (Iguania, Iguanidae) and *Pristidactylus achalensis* (Gallardo, 1964) (Iguania, Leiosaridae) (Higham et al., 2021), taxa employed as exemplars of generalized lizard ankle and tarsometatarsus structure (Brinkman, 1980; Rewcastle, 1980; Russell & Bauer, 2008), numerous differences in the osteology and arthrology of the ankle and tarsometatarsus were noted for *Gekko gecko*. The astragalocalcaneum bears a deep median hollow ventrally and exhibits a lateral process that is drawn out into a prominent, rectangular flange extending well beyond its fibular facet. Furthermore, the mesial aspect of the tibial facet of the astragalocalcaneum is excavated into a deep hollow that receives a projection of the distal end of the tibia, providing greater rigidity to this articulation. The fourth distal tarsal of *Gekko* is a robust, wedge-shaped bone that is elongated proximodistally and tapers distally. Its articulatory facets are deep, clearly defined, and contact with the third distal tarsal and the fourth and fifth metatarsals is more extensive than in *Iguana* and *Pristidactylus* (Higham et al., 2021), but its ventral peg is greatly reduced in size. The meniscus, intracapsular and extracapsular ligaments associated with the ankle joint are consistent in number and skeletal associations with those observed in *Iguana* and *Pristidactylus* (Higham et al., 2021), although their situation and courses are somewhat different because of differences in form and proportionality of their associated skeletal elements.

Among non-gekkotan lizards, the genus *Anolis* Daudin, 1802 (Family Anolidae—de Queiroz, 2022) has independently evolved adhesive toe pads (Losos, 2009). The anole adhesive system (Figure 1b,d) is regarded as being convergent with that of geckos (Autumn et al., 2002; Autumn & Peattie, 2002; Garner et al., 2021; Griffing et al., 2022; Hagey, Harte, et al., 2017; Hagey, Uyeda, et al., 2017; Irschick et al., 2005; Maderson, 1970; Russell & Garner, 2023), although there are clear differences in the form and arrangement of the adhesive setae (Ruibal & Ernst, 1965; Russell & Garner, 2023) of these two taxa. As members of the iguanian radiation, anoles are more closely related to *Iguana iguana* and *Pristidactylus achalensis*, the taxa employed by Higham et al. (2021) for comparison with ankle/tarsometatarsus structure (Higham et al., 2021), than they are to *Gekko gecko* (Gekkota, Gekkonidae).

Although the ecology and evolution of anoles have been extensively studied (Losos, 2009), relatively little is known about the biomechanical deployment of their convergently acquired adhesive toe pads (Garner et al., 2019), even though these are regarded as a

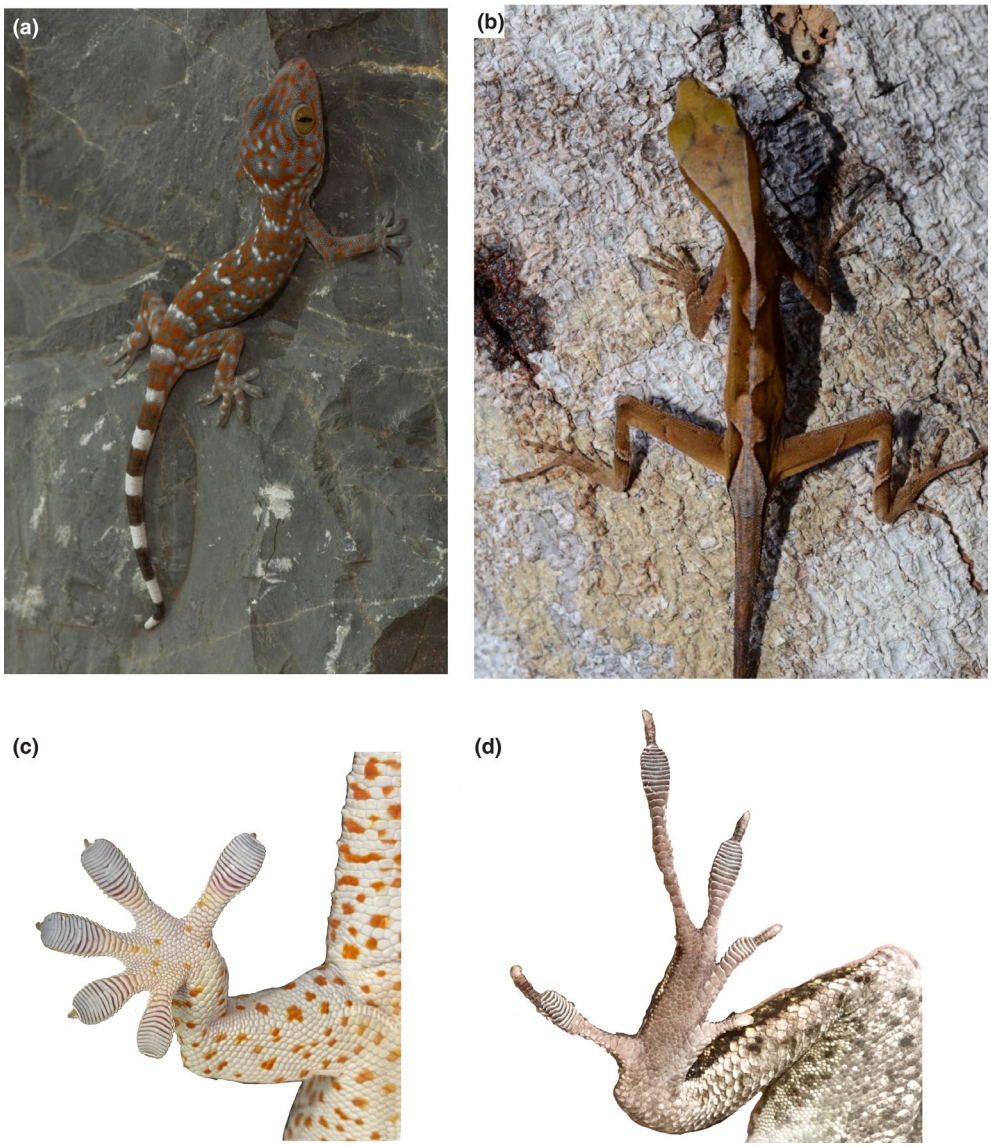

FIGURE 1 External pedal form of *Gekko* and *Anolis*. (a) *Gekko gecko* clinging to a vertical rock surface (photograph courtesy of Lee Grismer). Note the radiating symmetry of the digits of the right pes, the robust thigh and crus, and the short metapodial region of the hind foot. (b) *Anolis chrysolepis* clinging to a vertical rock surface (photograph by Tim Higham). Note the long metapodial region of the left pes, and the gracile thigh and crus. (c) Ventral view of the left pes of *Gekko gecko* clinging to a vertical glass surface (photograph by Tim Higham). The toe pads radiate about an arc and the adhesive surfaces are aligned adjacent to one another. (d) Ventral view of the right pes of *Anolis scriptus* clinging to a vertical glass surface (photograph courtesy of Colin Donihue). The metatarsal region is elongate and gracile. The toe pads on the elongated digits are staggered such that they do not lie adjacent to each other. Digit I lacks a definitive toe pad and Digit V arises far proximal to Digit IV. Digits I–IV deviate from the metapodial long axis at the metatarsophalangeal joints, the metatarsals being essentially parallel with one another.

key innovation of the genus (Losos, 2009; Miller & Stroud, 2022). Given that *Anolis* employs adhesively competent digits in locomotion (Garner et al., 2021), it is possible that pedal displacement patterns have converged upon those of geckos (Russell & Garner, 2023) in association with the governance of the adhesive mechanism. To explore this possibility, we investigate whether the ankle/tarsometatarsus structure of *Anolis* converges with that of geckos or retains features more akin to those of the ancestral lacertilian condition (Brinkman, 1980; Higham et al., 2021; Rewcastle, 1980). Unlike *Gekko gecko*, *Anolis* employs passive, rather than active, hyperextension of its toe pads upon release from the substratum (Russell & Bels, 2001). Its asymmetrical pes is rolled onto its medial border to effect toe pad detachment, representing retention of the pattern of digit release exhibited by lizards that ancestrally lack toe pads (Higham et al., 2017; Russell, 2002; Russell et al., 2015) and geckos with incipient, but adhesively competent (Russell & Garner, 2023), toe pads (Russell et al., 2015; Russell & Gamble, 2019).

The external morphological features of the pes of *Anolis* (Figure 1b,d) differ less from those of lizards in general than do those of geckos (Russell et al., 1997) (Figure 1a,c). *Anolis* exhibits

essentially parallel alignment of metatarsals I–IV, with these increasing in length across this series (Russell & Garner, 2023, fig. 1b), the digits deviating from the metatarsals at the metatarsophalangeal joints (Figure 1b,d). Such pedal configuration, along with the lack of active digital hyperextension (Russell & Bels, 2001), led us to predict that the osteological and arthrological features of the ankle joint and tarsometatarsus of *Anolis* would differ less from those of *Iguana* and *Pristidactylus* than do those of *Gekko* (Higham et al., 2021) and other pad-bearing geckos. Although interactions at the adhesive fibril/substratum interface are governed by specific physical principles (Russell & Garner, 2023), the mechanical ways in which these demands are met can differ (Gamble et al., 2012). Morphologies that function in much the same general way may result in features that are superficially similar but bear the evidence of precursory ancestral configuration (Clark & O'Connor, 2021). Indeed, Hagey, Harte, et al. (2017), in their comparison of the locomotor attributes of geckos and anoles, noted that although these two assemblages possess adhesive toe pads, their locomotor systems (as assessed by comparisons of both total limb length and the relative lengths of the individual limb sectors [brachium/thigh; antebrachium/crus; manus/pes]) seemingly complement their adhesive apparatus in different ways, with geckos having relatively shorter limbs (and limb segments) than anoles (Figure 1). Hagey, Harte, et al.'s (2017) conclusions, however, incorporate the unstated assumption that the mechanics of the individual sectors of the limbs are consistent for all of the taxa that they examined. Given that the pedal configuration of geckos (Figure 1a,c) differs markedly from that of other lizards (Russell et al., 1997) and the morphology of the ankle joint and the movements of the pes enabled by this (Higham et al., 2021) are unusual among limbed squamates, we herein examine ankle and tarsometatarsus structure of geckos and anoles in greater detail to determine whether the mechanics of the pes differs between these two clades. Our findings will provide anatomical information pertinent to the determination of whether the ecomechanics of the deployment of adhesive toe pads (Figure 1b,d) differs in these two lineages, thereby shedding more light on why there may be "more than one way to climb a tree" (Hagey, Harte, et al., 2017).

2 | MATERIALS AND METHODS

To explore the general aspects of the configuration of the anoline mesotarsal joint and tarsometatarsus, we examined its structure in skeletally mature individuals of *Iguana iguana* ($n = 9$ ♂; 0♀), *Pristidactylus achalensis* ($n = 13$♂; 5♀), two species of *Anolis* [*Anolis garmani* Stejneger, 1899 ($n = 13$♂; 8♀), *Anolis equestris* Merrem, 1820 ($n = 1$♂; 0♀)], and *Gekko gecko* ($n = 8$♂; 3♀). Investigation for all of these taxa involved dissection, examination of prepared skeletons (Russell & Bauer, 2008) and cleared and stained specimens, and radiographic imaging (using a Hewlett-Packard Faxitron Model 4380N x-ray system and Polaroid Type 55 Positive/Negative (P/N) black and white film). Additionally, for *Pristidactylus achalensis*, *Anolis garmani*, *Anolis equestris*, and *Gekko gecko*, scanning electron microscopy (SEM) was employed to visualize these anatomical components as these species are of sufficiently small adult size to permit SEM exploration and imaging of the fully articulated ankle and tarsometatarsus. To achieve this, the crus and pes were excised from formalin-fixed, ethanol-preserved specimens, and the integument and musculature were removed by dissection, retaining the ligaments that bind the skeletal elements together. These preparations were dehydrated by immersion in a sequential series of ethanol baths (70%; 90%; 96%; 100%), air dried, affixed to stubs with high purity colloidal silver paste, and sputter coated with gold to a thickness of ~20 ηm, using a Semprep2 sputter coater, and viewed with a Hitachi S-450 SEM in the Microscopy and Imaging Facility, Cumming School of Medicine, University of Calgary. Photomicrographs of appropriate regions of the preparations were amalgamated into composite images. All specimens were from the personal collection of APR, having been salvaged from use in previous studies (under the auspices of Animal Care protocols (BI 2005-22, BI 2008-24) issued to APR by the University of Calgary Animal Care Committee).

Additionally, to ensure that the ankle and tarsometatarsal skeletal configuration of *Gekko gecko* is not atypical of geckos in general, the distal part of the crus and its associated pes of ethanol-preserved specimens of 43 species of gecko, representing 33 genera (Table 1), were micro-computer tomographically (μCT) scanned with Scanco 35 and Scanco 40 instruments (at a minimum of 5 μm resolution) in the MicroCT Laboratory, Cumming School of Medicine, University of Calgary. Specimens for μCT were wrapped in cheesecloth moistened with ethanol and encased in Styrofoam to prevent movement and rotation of the specimen and ethanol evaporation from the sample chamber during long scanning periods (about 1 h per foot). The species scanned provide broad representation across the gekkotan phylogeny (Table 1) and include ancestrally padless, toe pad-bearing, and secondarily padless taxa. Clade assignment and toe pad condition follow the designations of Gamble et al. (2012, fig. 1). We employ this phylogenetic arrangement rather than that of Russell and Gamble (2019) because the clades in the former publication are identified by letter (Table 1) whereas the phylogeny depicted by Russell and Gamble (2019) leaves many clades unlabelled. The positioning of some genera within these two representations of gekkotan phylogeny differs slightly, but toe pad evolutionary state is identical for all but one genus (*Ptenopus* Gray, 1866) and does not affect our interpretations.

3 | RESULTS

The morphology of the astragalocalcaneum (hereafter referred to as AC) and fourth distal tarsal (hereafter distal tarsals are referred to as DT3 and DT4, as appropriate) of *Iguana iguana*, *Pristidactylus achalensis*, and *Gekko gecko* was described in detail and figured by Higham et al. (2021: pp. 1506–1511, Figures 2–5 and 8). These descriptions are not repeated here. To complete coverage of the tarsometatarsus for these three species, we describe the morphology of the remaining DTs and the metatarsals (hereafter metatarsals are referred to as MT I, MT II, MT III, MT IV, MT V, as appropriate according to digital ray designation). Subsequently, we provide a brief survey of

TABLE 1 Preserved specimens of geckos for which the ankle region and associated pes were micro-computer tomographically (μCT) imaged.

Clade (see Gamble et al., 2012)	Species	Toe pad state	Specimen information
C Carphodactylidae + Pygopodidae	*Nephrurus asper* Günther, 1876	Ancestrally padless	APR
F Diplodactylidae	*Rhacodactylus auriculatus* (Bavay, 1869)	Pad-bearing	APR
	Strophurus Fitzinger, 1843 sp.	Pad-bearing	APR
	Diplodactylus Gray, 1832 sp.	Pad-bearing	APR
H Eublepharidae	*Coleonyx mitratus* (Peters, 1863)	Ancestrally padless	APR
	Eublepharis macularius (Blyth, 1854)	Ancestrally padless	APR
J Sphaerodactylidae	*Teratoscincus* Strauch, 1863 sp.	Ancestrally padless	APR
	Gonatodes Fitzinger, 1843 sp.		TG 1729
L Phyllodactylidae	*Thecadactylus* Goldfuss, 1820 sp.	Pad-bearing	APR
N Gekkonidae Bent-toed and *Hemidactylus* clade	*Stenodactylus petrii* Anderson, 1896	Ancestrally padless	CAS 138984
	Stenodactylus sthenodactylus (Lichtenstein, 1823)	Ancestrally padless	APR
	Agamura persica (Duméril, 1856)	Ancestrally padless	CAS 140554
	Bunopus tuberculatus Blanford, 1874	Ancestrally padless	CAS 148556
	Cyrtopodion scabrum (Heyden, 1827)	Ancestrally padless	APR
	Cyrtodactylus astrum Grismer, Wood, Quah, Anuar, Muin, Sumontha, Ahmad, Bauer, Wangkulangkul, Grismer & Pauwels, 2012	Ancestrally padless	LSU 10023
	Cyrtodactylus consobrinus (Peters, 1871)	Ancestrally padless	LSU 11269
	Cyrtodactylus macrotuberculatus Grismer & Ahmad, 2008	Ancestrally padless	LSU 9981
	Cyrtodactylus quadrivirgatus Taylor, 1962	Ancestrally padless	LSU 12234
	Cyrtodactylus Gray, 1827 sp.	Ancestrally padless	CAS 259981
	Hemidactylus frenatus Duméril & Bibron, 1836	Pad-bearing	LSU 7644
O Gekkonidae Afro-Malagasy clade	*Nactus pelagicus* (Girard, 1858)	Ancestrally padless	CAS 155760
	Nactus Kluge, 1983 sp.	Ancestrally padless	APR
	Dixonius siamensis (Boulenger, 1899)	Pad-bearing	APR
	Heteronotia binoei (Gray, 1845)	Ancestrally padless	APR
	Lepidodactylus Fitzinger, 1843 sp.	Pad-bearing	APR
	Gekko browni (Russell, 1979)	Pad-bearing	LSU 9112
	Gekko kuhli (Stejneger, 1902)	Pad-bearing	APR
	Gekko Laurenti, 1768 sp.	Pad-bearing	APR
	Perochirus ateles (Duméril, 1856)	Pad-bearing	CAS 159786
	Hemiphyllodactylus titiwangsaensis Zug, 2010	Pad-bearing	LSU 7209
	Gehyra oceanica (Lesson, 1830)	Pad-bearing	CAS 152379
	Gehyra Gray, 1834 sp.	Pad-bearing	APR
	Ptenopus Gray, 1866 sp.	Ancestrally padless	APR
	Uroplatus henkeli Böhme & Ibisch, 1990	Pad-bearing	APR
	Uroplatus lineatus (Duméril & Bibron, 1836)	Pad-bearing	APR
	Uroplatus sikorae Boettger, 1913	Pad-bearing	APR
	Uroplatus A.M.C. Dumeril, 1806 sp.	Pad-bearing	APR
	Ailuronyx seychellensis (Duméril & Bibron, 1836)	Pad-bearing	APR
	Lygodactylus Gray, 1864 sp.	Pad-bearing	APR
	Phelsuma Gray, 1825 sp.	Pad-bearing	APR
	Geckolepis Grandidier, 1867 sp.	Pad-bearing	APR
	Homopholis Boulenger, 1885 sp.	Pad-bearing	APR

(Continues)

TABLE 1 (Continued)

Clade (see Gamble et al., 2012)	Species	Toe pad state	Specimen information
	Rhoptropus afer Peters, 1869	Pad-bearing	APR
	Rhoptropus bradfieldi Hewitt, 1935	Pad-bearing	APR
	Chondrodactylus angulifer Peters, 1870	Secondarily padless	APR
	Chondrodactylus bibronii (Smith, 1846)	Pad-bearing	APR
	Pachydactylus punctatus Peters, 1854	Pad-bearing	APR
	Pachydactylus rangei (Andersson, 1908)	Secondarily padless	APR

Note: Species names in the table occur in the order of appearance of the genera in the branching sequence of the cladogram depicted in figure 1 of Gamble et al. (2012). Clade membership and toe pad state, as per Gamble et al. (2012) are indicated.

Abbreviations: APR, personal collection of Anthony Russell; CAS, California Academy of Sciences; LSU, La Sierra University; TG, personal collection of Tony Gamble.

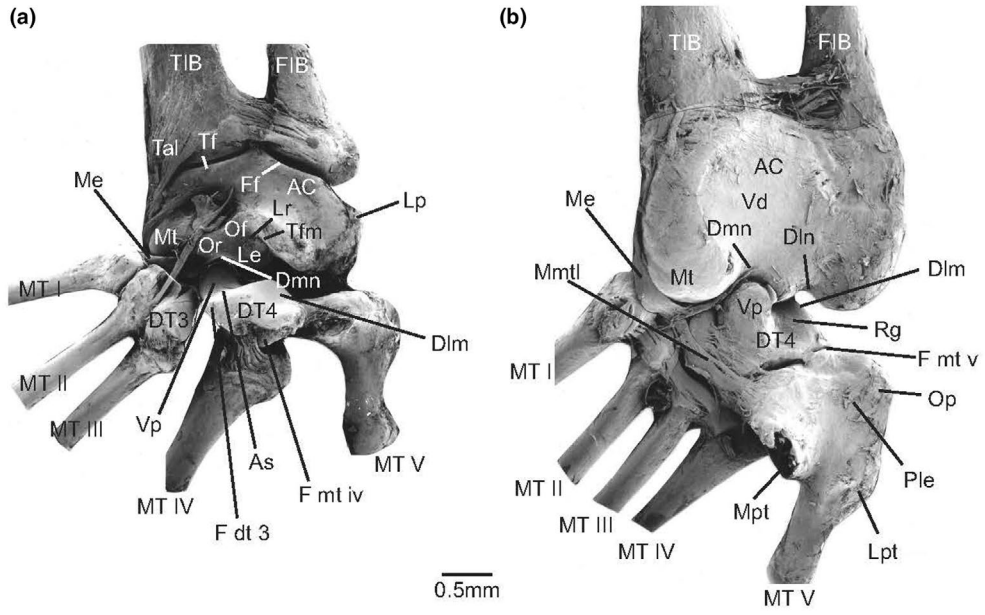

FIGURE 2 (a) Dorsal and (b) ventral views (as assembled from composite scanning electron miscroscopic [SEM] images) of ligamentous preparations of the skeleton of the left (a) and right (b) ankle and tarsometatarsal region of the leiosaurid iguanian *Pristidactylus achalensis*. Skeletal elements: AC, astragalocalcaneum; DT3, third distal tarsal; DT4, fourth distal tarsal; FIB, fibula; MT I–MT V, first to fifth metatarsals; TIB, tibia. Features of the astragalocalcaneum: Dln, distolateral notch; Dmn, distomesial notch; Ff, fibular facet; Le, lateral expansion; Lp, lateral process; Lr, lateral rim of tarsal facet; Mt, mesial tubercle; Of, oblique furrow; Or, oblique ridge; Tf, tibial facet; Tfm, tarsal facet margin; Vd, ventral depression. Features of the fourth distal tarsal: As, articular surface for contact with the distomesial notch of the astragalocalcaneum; Dlm, distolateral margin; F dt 3, facet for articulation with the third distal tarsal; F mt iv, facet for articulation with the fourth metatarsal; F mt v, facet for articulation with the fifth metatarsal; Rg, ridge and groove; Vp, ventral peg. Features of the fifth metatarsal: Lpt, lateral plantar tubercle; Mpt, mesial plantar tubercle; Op, outer process; Ple, proximolateral expansion. Soft tissue structures: Me, meniscus; Mmtl, meniscometatarsal ligaments; Tal, tibioastragalar ligament.

the osteology of the ankle and tarsometatarsus of a broader array of geckos to assess basic configuration. Finally, we describe the AC and tarsometatarsus (DTs and MTs) of *Anolis* and explore their arthrology.

3.1 | Osteology of the tarsometarsus of *Iguana and Prisidactylus*

The morphology of the tarsals of *Iguana* and *Pristidactylus* (Figure 2) is essentially identical, and no features of DT3 or DT4 distinguish *Pristidactylus* from the former.

Iguana and *Pristidactylus* lack DT2 (this absence being a feature of the Lacertilia—Russell & Bauer, 2008), the distal tarsal row thus consisting of only DT3 and DT4. DT3 (Figure 2a) is much smaller than DT4. It abuts the proximal ends of MT II and MT III distally and DT4 proximally. It is broadest proximodorsally and narrow both distally and ventrally, intervening in a wedge-like fashion between the proximal ends of MT II and MT III. On its proximal end there is a ligament scar and onto this, and the proximal head of MT II, attach astragalometatarsal ligaments (Figure 3) typical of the lacertilian mesotarsal joint (see below).

The proximolateral facet of DT3, for articulation with the DT4, is convex and matches the distomesial concavity of the latter

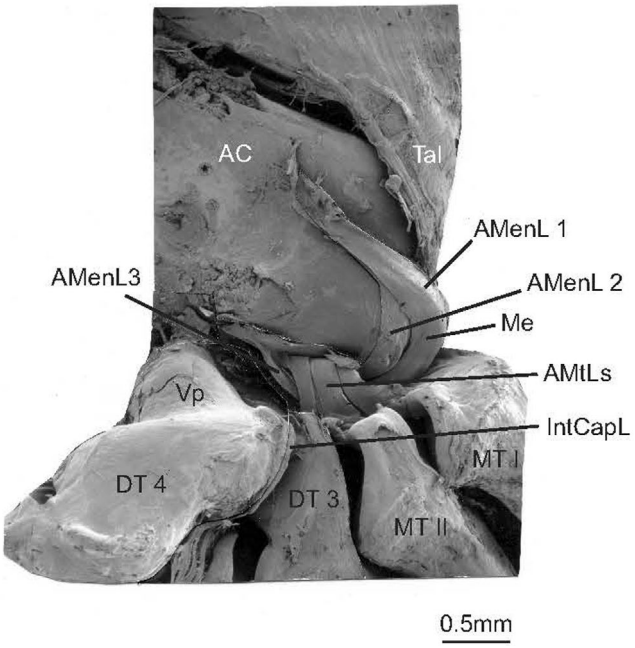

FIGURE 3 Scanning electron microscopic (SEM) composite image of the dorsal aspect of the mesial region of the right ankle joint of the iguanid iguanian *Iguana iguana* showing the meniscal and metatarsal ligaments. Soft tissue structures: AMenL 1–AmenL3, first, second, and third astragalomeniscal ligaments; AMtLs, astragalometatarsal ligaments; IntCapL, intracapsular ligaments. Other abbreviations as in Figure 2.

(Figures 2a and 3). The distomesial facet, for articulation with the proximolateral aspect of MT II (Figures 2a and 3), and the distal facet, where it abuts the proximal aspect of MT III (Figures 2a and 3), are both basically planar.

MTI, MT III, and MT IV of *Iguana* and *Pristidactylus* (Figures 2 and 4) have a similar morphology and are largely indistinguishable. *Pristidactylus* deviates slightly from *Iguana* in the morphology of MT II and MT V, but these differences do not alter the arrangement between the DTs and the MTs. In *Pristidactylus*, the proximal end of MT II (Figures 2 and 4) is rounder than that of *Iguana* (Figure 3), the articulatory facets are not oriented as steeply, the curvature of the shaft is somewhat greater, and the proximal end is relatively broader ventrally. On MT V, the mesial and lateral tubercles of *Pristidactylus* (Figure 4) do not exhibit as pronounced a curvature as they do in *Iguana* (Russell & Bauer, 2008, fig.1.20b).

Both *Iguana* and *Pristidactylus* exhibit an imbricate metatarsus (Figures 2a and 3), the proximal ends overlapping and shaping the metatarsus into a transverse arch (Russell & Bauer, 2008, fig. 1.20). The proximal ends of MT III and MT IV are similar in shape (Figures 2 and 4), being flattened and expanded, the opposing facets of the expansions of each being directed ventrolaterally and dorsomesially (Figure 2a,b). The proximal end of MT III partially overlies that of MT IV in dorsal view (Figure 2a). The proximal end of MT II is markedly wedge-shaped (Figure 2a), with its apex directed proximally (Figures 2a and 4) and is also broader dorsally than ventrally (Figure 2b), so that in the ventral

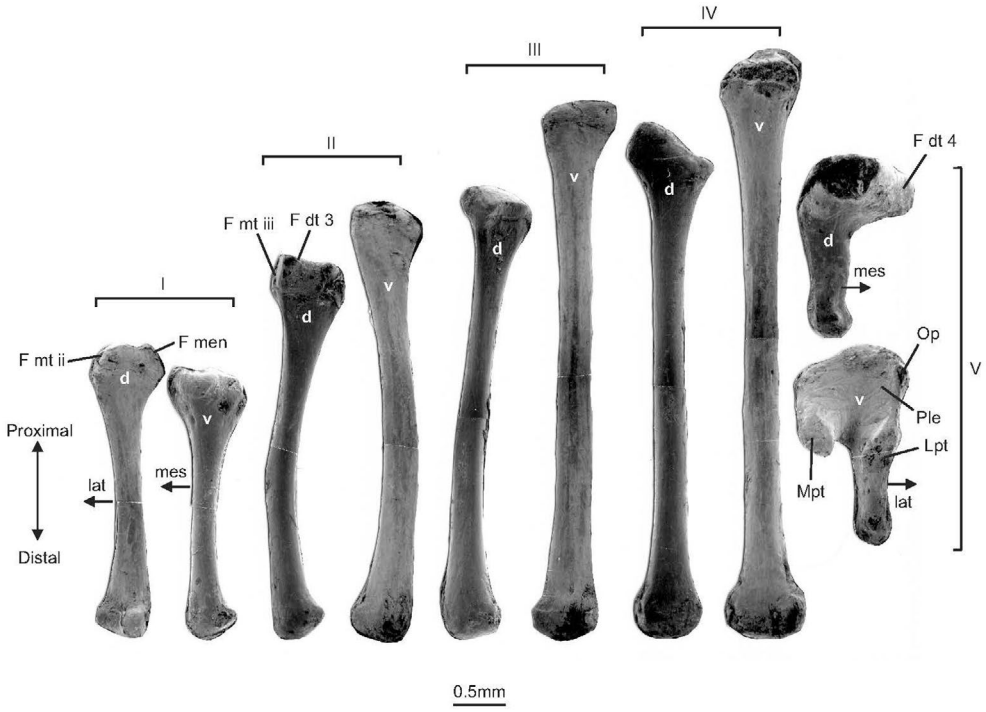

FIGURE 4 Scanning electron microscopic (SEM) composite images of the metatarsals of the right pes of *Pristidactylus achalensis* in dorsal, d and ventral, v views. For each metatarsal pair (dorsal and ventral views) the two images are of elements from different individuals, hence their difference in absolute size. Lateral and mesial aspects are indicated by "Lat" and "Mes," respectively. Abbreviations for features of the fifth metatarsal are as in Figure 2.

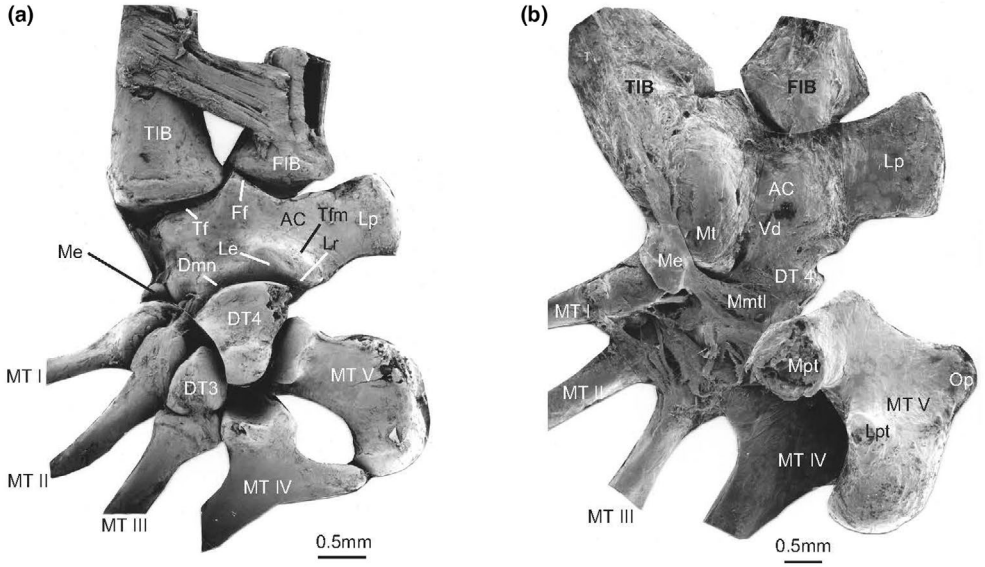

FIGURE 5 Scanning electron microscopic (SEM) composite images of dorsal (a) and ventral (b) views of ligamentous preparations of the left (a) and right (b) ankle and tarsometatarsal region of the gekkonid gekkotan *Gekko gecko*. All abbreviations are as in Figure 2.

view of the articulated metatarsus it is nearly obscured by DT3 and the proximal end of MT I (Russell & Bauer, 2008, fig. 1.20). MT II articulates laterally chiefly with DT3 (Figure 2a) and there is only a very limited contact between the proximal ends of MTs II and III (Figures 2a and 3). Mesially, MT II articulates with the proximal end of MT I (Figures 2 and 4). Because the proximal end of MT II is wedge-shaped and broader dorsally than ventrally, it lies dorsal to MT I and MT III (Figure 2a), its shape and position being analogous to the keystone of an arch (Rewcastle, 1980; Russell & Bauer, 2008). The proximal end of MT I is expanded and bears two large articulatory facets (Figures 2a,b and 4); the lateral one has a flat surface (Figure 2a) and contacts the proximal end of MT II (Figure 2a), the proximolateral one articulates, via intervention of the cartilaginous meniscus (Figures 2a,b–4), with the distomesial margin of the AC.

In both *Pristidactylus* and *Iguana*, the relative proportions of the MTs are similar (Table 2), and the distal tips of the first three lie on a straight, oblique line (Russell & Bauer, 2008, fig. 1.19) in the intact pes. The greatest discrepancy in length between adjacent metatarsals is that between MT I and MT II (Figure 4; Table 2). Comparison of the lengths of MT I and MT IV reveals that MT IV is almost twice as long as MT I (Table 2).

The shafts of the first four MTs are smooth (Figure 4) and have an oval cross-section with its long axis oriented mesiolaterally. The distal ends of the shafts of MT II and MT III are offset somewhat mesially (Figure 4) by virtue of their diaphyseal curvature (Figure 4). The distal ends of the MTs are expanded into broad, condyloid facets forming the proximal surfaces of the metatarsophalangeal articulations (Figure 4). The distal condyle of MT I is asymmetrical (Figure 4), its lateral area being larger than its mesial one (Figure 4). The ventral margin of the condyle is divided by a prominent notch (Figure 4) into which slots the ventral tongue of the first phalanx of Digit I. The hinge axis of this articulation is not perpendicular to the long axis of the first digit, due to the asymmetry of the joint (Figure 4). The terminal condyles of MTs II, III, and IV are increasingly less asymmetrical (Figure 4). The distal condyles of MT III and MT IV are bulbous, subhemispherical, somewhat depressed (Figure 4), and have a greater area than the proximal facets of the corresponding first phalanges, which are concave and not divided by a dorsoventral ridge. Digits III and, especially, IV can be markedly abducted away from the long axis of the foot (Robinson, 1975) (Figure 1b,d), such movements being permitted by the morphology of the metatarsophalangeal joints, which are essentially unicondylar rather than ginglymoid (Figure 4).

MT V of both *Iguana* and *Pristidactylus* is similar. Its hooked shape, expanded proximal end, and short shaft render it markedly different from the other MTs (Figures 2a,b and 4). Its articulation with DT4 is offset mesially from the shaft (Figure 2b) due to mediolateral hooking of MT V. MT V encroaches farther proximally than the other MTs, and its chief proximal articulation is with DT4

TABLE 2 Proportional lengths of the metatarsals of *Pristidactylus achalensis*, *Anolis garmani*, and *Gekko gecko*.

	Pristidactylus achalensis	*Gekko gecko*	*Anolis garmani*
MT II % MT I	151.4	139.9	211.0
MT III % MT II	114.6	95.9	112.8
MT IV % MT III	111.1	75.0	111.3
MT IV % MT I	192.9	100.6	265.0

Note: The first three rows express the relative length of the lateralmost metatarsal of an adjacent couple (e.g., the length of MT II as a percentage of the length of MT I) relative to its more medial counterpart. Numbers greater than 100 indicate that the more lateral member of the pair is longer than the more medial member (and accordingly numbers less than 100 indicate that it is shorter). The fourth row compares the relative length of MT IV to that of MT I and indicates relative length discrepancy across the first four metatarsals.

(Figure 2a,b). The distal end of MT V differs from that of the first four (Figures 2a,b and 4). The terminal condyle, articulating with the first, phalanx of digit five, is convex and essentially hemispherical, lacks a ventral notch (Figures 2b and 4), and is also slightly asymmetrical, being cut away laterally (Figure 4), promoting the lateral deviation of Digit V from the remainder of the digital rays (Figure 1d). The ball and socket nature of this joint also allows rotation of Digit V about its long axis (Russell & Bauer, 2008).

The plantar surface of the proximal end of MT V (Figures 2b and 4) bears prominent tubercles. The lateral plantar tubercle (Figures 2b and 4) is situated on the lateral margin of the plantar surface, at the point where the shaft meets the proximal end. Lying opposite this is the mesial plantar tubercle (Figures 2b and 4). The two tubercles arch toward one another, forming the margins of an open canal within which the origin tendon of one of the astragalocalcaneal heads of the *m. flexor digitorum longus* is situated (Russell & Bauer, 2008, fig. 1.48b). The mesial plantar tubercle is prolonged toward the proximomesial margin of the ventral surface (Figures 2b and 4). The proximolateral corner of the proximal end of MT V constitutes the proximolateral expansion (Figures 2b and 4) (Goodrich, 1916; Robinson, 1975) which, at its extreme proximolateral corner, bears the outer process (Figures 2b and 4). The proximal end of MT V is markedly concave ventrally (Figures 2b and 4).

3.2 | Osteology of the tarsometatarsus of *Gekko gecko*

Higham et al. (2021) noted that DT3 of *Gekko gecko* articulates with the distomesial face of DT4 and that the proximal heads of all five metatarsals are closely interlinked (Figure 5). The arrangement of DT4 and DT3, and their intimate connections with the proximal heads of all five MTs, creates a linked set of elements that can be displaced as a unit on the smooth, rounded articulation between the broad proximodorsal facet of DT4 and the expansive distomesial notch of the AC (Figure 5).

The proximal head of MT I of *Gekko gecko* is flattened on its lateral face (Figures 5a and 6), whereby it makes broad contact with the planar medial facet of the proximal head of MT II (Figure 5a,b). The first two MTs constitute a unit that articulates proximally with the distomesial aspect of the AC (Figure 5a), proximolaterally (via the proximolateral face of MT I) with the meniscus that lies at the distomesial margin of the AC (Figure 5a,b), and laterally (via the planar lateral facet of MT II) with the broad medial aspect of DT3 and the proximomesial aspect of DT 4 (Figure 5a).

Compared to MT III of *Pristidactylus* (Figures 2a and 4) and *Iguana*, the proximal head of MT III of *Gekko* is displaced distally (Figure 5a), and articulatory contact between MT II and MT III is minimal. The imbrication of the proximal heads of the first three MTs is less evident in *Gekko* (Figure 5a) than it is in *Pristidactylus* (Figure 2a) and *Iguana*. The proximal head of MT III of *Gekko* bears a broad proximomesial facet for articulation with DT3 and a broad, laterally-facing proximolateral facet for articulation with MT IV (Figures 5a and 6). Proximal contact between the heads of the MTs is thus more extensive and continuous in *Gekko* (Figure 5a) than it is in *Pristidactylus* (Figure 2a) and *Iguana*.

The diaphysis of MT I of *Gekko gecko* is curved such that its proximal head is medially displaced relative to its distal head (Figure 6). Its proximal head is compressed mediolaterally so that its articulatory facet for contact with MT II is offset (Figure 6). The shaft is smooth and narrowest at its midpoint. MT II also has a unicondylar distal articulatory surface (Figure 6) and its shaft is slightly bowed, but less so than MT I (Figure 6). MT III is of approximately equal length to MT II (Table 2), and both are appreciably longer than MT I (Table 2). The proximal end of MT III bears prominent facets for articulation with MT IV laterally and DT3 mesially (Figure 6). The shaft of MT III is essentially straight (Figure 6) and bears a broad, unicondylar, globose distal articulatory surface (Figure 6). MT III is essentially excluded from contact with DT4 by the broad medial encroachment of the proximal head of MT IV (Figure 5a).

MT IV of *Gekko gecko* (Figure 6) departs markedly in morphology from that of *Pristidactylus* (Figure 4), *Iguana*, and other non-gekkotan lizards by being relatively short (shorter than MT III—Table 2), robust rather than gracile, and bearing a broadly expanded, morphologically elaborate proximal head. The latter is extended into an attenuated lateral wing (Figure 6) for contact with the distomesial aspect of MT V (Figure 5a), a proximally directed process (Figure 6), a mesial flange (Figure 6) that envelops the tapered distodorsal extension of DT4 (Figure 5a) and contacts DT3 (Figure 5a), and a mesial facet for contact with MT III (Figures 5 and 6). The proximal end of MT IV thus forms a yoke uniting MT V, DT4, DT3, and MT III into a unified entity (Figures 5a and 6). Ventrally, the proximal aspect of MT IV bears a dish-like recess. The distal articulatory surface of MT IV is broad, globular, unicondylar, and slightly offset laterally (Figure 6).

MT V of *Gekko gecko* is robust and proximally markedly hooked (Figures 5 and 6). Its proximal end is conspicuously and extensively sculpted (Figures 5 and 6) and its shaft is relatively short in comparison to the mediolateral width of this element (Figures 5 and 6). Proximomesially, it bears a prominent facet for contact with DT4 (Figure 6) and another for contact with MT IV (Figure 6). Its outer process (Figure 6) extends laterally away from the proximal aspect of the element, its lateralmost point being aligned with the lateral extremity of the lateral process of the AC (Figure 5). The lateral and mesial plantar tubercles are prominent (Figures 5b and 6), straddling a broad channel on the ventral surface of MT V. In the intact tarsometatarsus, MT V lies ventral to MT IV (Figure 5b) and its contact with MT IV and DT4 is such that any displacement of it relative to the astragalocalcaneum will result in displacement of the tarsometatarsus as a whole.

3.3 | Comparative survey of the osteology of the ankle and tarsometatarsus of geckos

The most visually evident derived features of the intact ankle joint and tarsometatarsus of *Gekko gecko* (Higham et al., 2021 and data

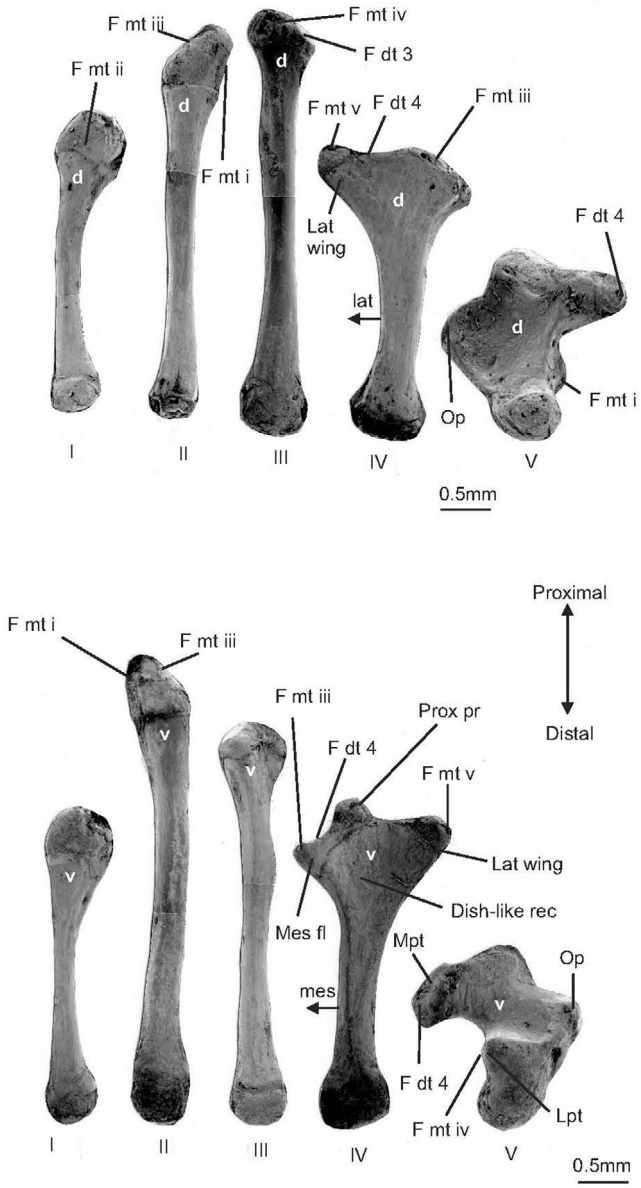

FIGURE 6 Scanning electron microscopic (SEM) composite images of the metatarsals of the right pes of *Gekko gecko* in dorsal, d and ventral, v views. For each metatarsal pair (dorsal and ventral views) the two images are of elements from different individuals, hence their difference in absolute size. Metatarsals are numbered I–V, indicative of digital ray identity. Lateral and mesial aspects are indicated by "Lat" and "Mes," respectively. Dish-like rec, Dish-like recess on the ventral aspect of the proximal extremity of the fourth metatarsal; F dt 3, F dt 4, facet for articulation with the third and fourth distal tarsals, respectively; F mt iii, F mt iv, F mt v, facet for articulation with the third, fourth, and fifth metatarsals, respectively; Lat f, lateral facet; Lat wing, lateral wing of the fourth metatarsal; Mes f, mesial facet; Mes fl, mesial flange of the fourth metatarsal; Prox pr, proximal process of the fourth metatarsal. All other abbreviations as in Figure 2.

presented above—Figure 5), when compared to the more widespread and generalized condition of lizards (Rewcastle, 1980) are as follows: (i) A prominent lateral process on the AC; (ii) a deep tibial facet on the proximomedial extremity of the AC for reception of the tibia; (iii) a robust, distally-tapering DT4 that affords extensive contact with the proximal ends of MT IV and MT V, which are themselves yoked together; (iv) a short-shafted, robust and highly-sculpted MT V; (v) a forseshortened MT IV; and (vi) a broadened proximal head of MT IV that contacts MT III, MT V, and DT4. To contextualize our comparison of ankle and tarsometatarsus structure between *Gekko* and *Anolis* we needed to establish whether the configuration in *Gekko* was not atypical of geckos in general. To accomplish this we surveyed general qualitative aspects of the ankle and tarsometatarsus across a broad representation of geckos (Table 1). Consideration of phylogenetic patterns of the evolution of quantitative traits among geckos will be addressed in a subsequent study.

Our survey of ankle joint and tarsometatarsus configuration of intact geckos (Figures 7 and 8) revealed a great deal of similarity across all families (we use the term geckos here to refer to all gekkotan families except the effectively limbless pygopodids). The presence of all six features outlined above is evident in most of the taxa examined (Figures 7 and 8; Table 1). The ancestrally padless carphodactylid *Nephrurus* Günther, 1876 (Figure 7a) has only a moderately expanded proximal head of MT IV, but otherwise exhibits all of the aforementioned features. This is also the case for the pad-bearing diplodactylids *Rhacodactylus* Fitzinger, 1843 (Figure 7b) and *Diplodactylus* Gray, 1832 (Figure 7c). The ancestrally padless eublepharid (Figure 7d) and sphaerodactylids (Figure 7e,f) all exhibit all six of the features outlined above, as does the pad-bearing phyllodactylid *Thecadactylus* (Houttuyn, 1782) (Figure 7g). Thus, the more basal gecko lineages (Gamble et al., 2012, fig. 1; Russell & Gamble, 2019, fig. 1) possess a *Gekko*-type ankle and tarsometatarsus (Higham et al., 2021 and data presented above), whether or not they possess adhesive toe pads. The form of MT IV is the most variable of the listed osteological attributes.

Among the Gekkonidae there are some taxa that exhibit ankle and tarsometatarsus morphology with some aspects of similarity to non-gekkotan lizards (as depicted here for *Pristidactylus achalensis*—Figures 2 and 4). The ancestrally padless *Stenodactylus* Fitzinger, 1826 (Figure 7h) and the ancestrally (Gamble et al., 2012) or secondarily (Russell & Gamble, 2019) padless *Ptenopus* (Figure 8d) have long, slender MTs, the fourth of which is essentially of equal length to MT III. Furthermore, the proximal head of MT IV of *Ptenopus* is not greatly expanded and MT V is less robust than in other geckos and its shaft is relatively long (Figure 8d). Both *Stenodactylus* and *Ptenopus* are terrestrial sand-dwellers. Converging on these in some respects are the secondarily padless, psammophilous *Chondrodactylus angulifer* Peters, 1870 and *Pachydactylus rangei* (Andersson, 1908) (Figure 8i,k), in which MT IV is of approximately equal length to MT III. In most other respects, however, the morphology of the ankle region and tarsometatarsus in these taxa corresponds quite closely to that of other gekkonids (Figures 7i–l and 8a–c,f–h,j), although the lateral process of the AC in *Stenodactylus* is relatively small. There is still much to be learned about variation in ankle and tarsometatarsus structure within the Gekkota and the possible ecomechanical implications of this.

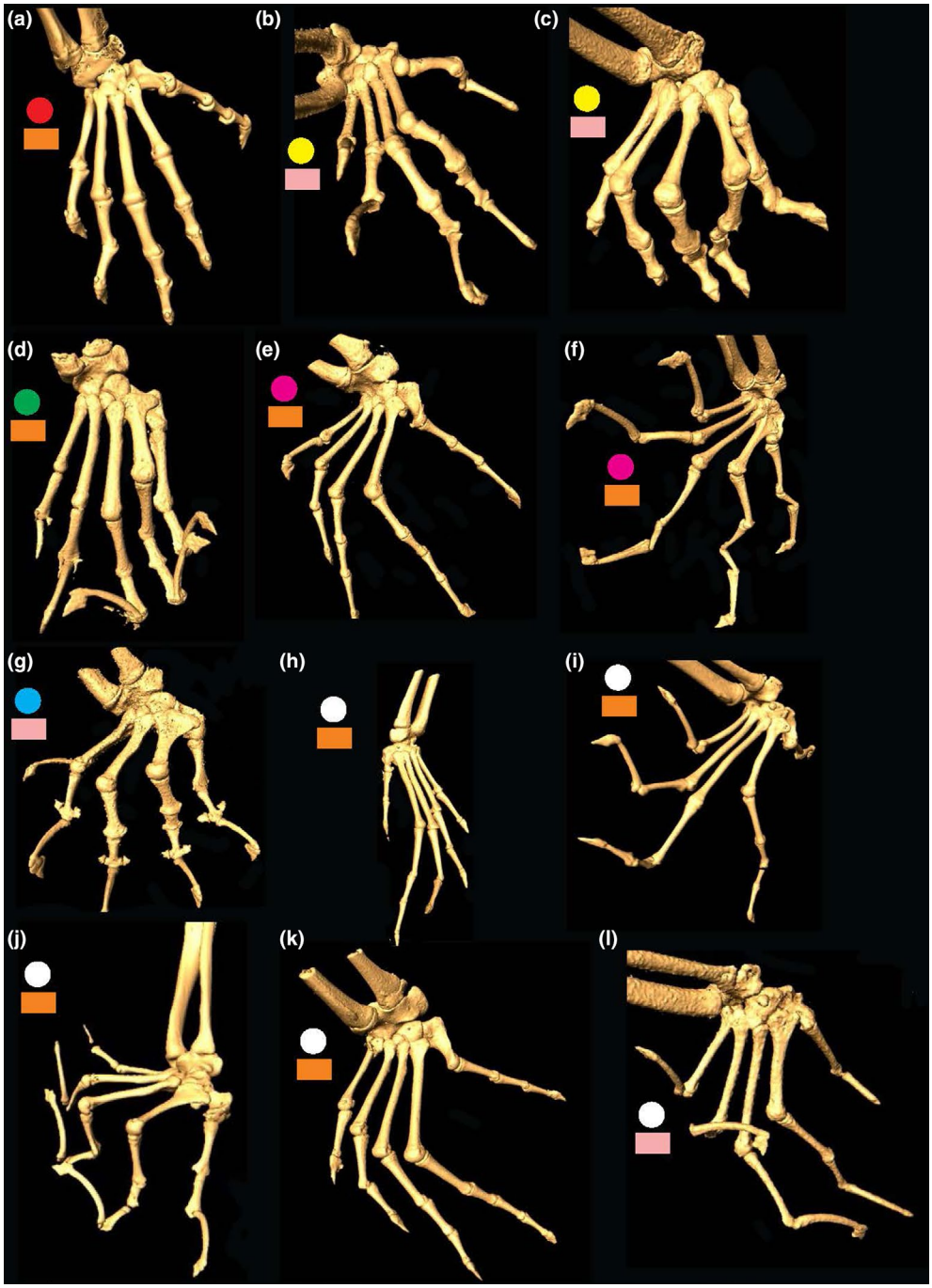

FIGURE 7 Micro-computed tomographic scan reconstructions of the lower crus and pedal regions of selected gekkotan lizards. All panels except (h) are of the left appendage; colored circles indicate family membership: Red, Carphodactylidae; Yellow, Diplodactylidae; Green, Eublepharidae; Mauve, Sphaerodactylidae; Blue, Phyllodactylidae; White, Gekkonidae. Colored rectangles indicate toe pad condition: Orange, ancestrally padless; Pink, pad-bearing. Taxa in this figure belong to clades C, F, H, J, L and N depicted in figure 1 of Gamble et al. (2012)—see Table 1 for details. Species depicted are as follows: (a) *Nephrurus* sp.; (b) *Rhacodactylus auriculatus*; (c) *Diplodactylus* sp., (d) *Eublepharis macularius*; (e) *Teratoscincus* sp., (f) *Gonatodes* sp., (g) *Thecadactylus* sp., (h) *Stenodactylus petrii*, (i) *Agamura persica*, (j) *Bunopus tuberculatus*; (k) *Cyrtodactylus macrotuberculatus*, (l) *Hemidactylus frenatus*.

3.4 | Osteology and arthrology of the ankle and tarsometatarsus of *Anolis*

The AC of *Anolis* (Figures 9 and 10) is depressed and firmly attached to the tibia and fibula. It has a width (w) to length (l) ratio of approximately 1.6:1. This is slightly greater than the w:l ratio of 1.5 for *Iguana* and 1.4 for *Gekko* (Higham et al., 2021). Proximally, the articulatory facets almost abut one another, save for an intervening narrow ridge of bone (Figure 9). The tibia and fibula approach one another more closely on the ventral surface than they do dorsally

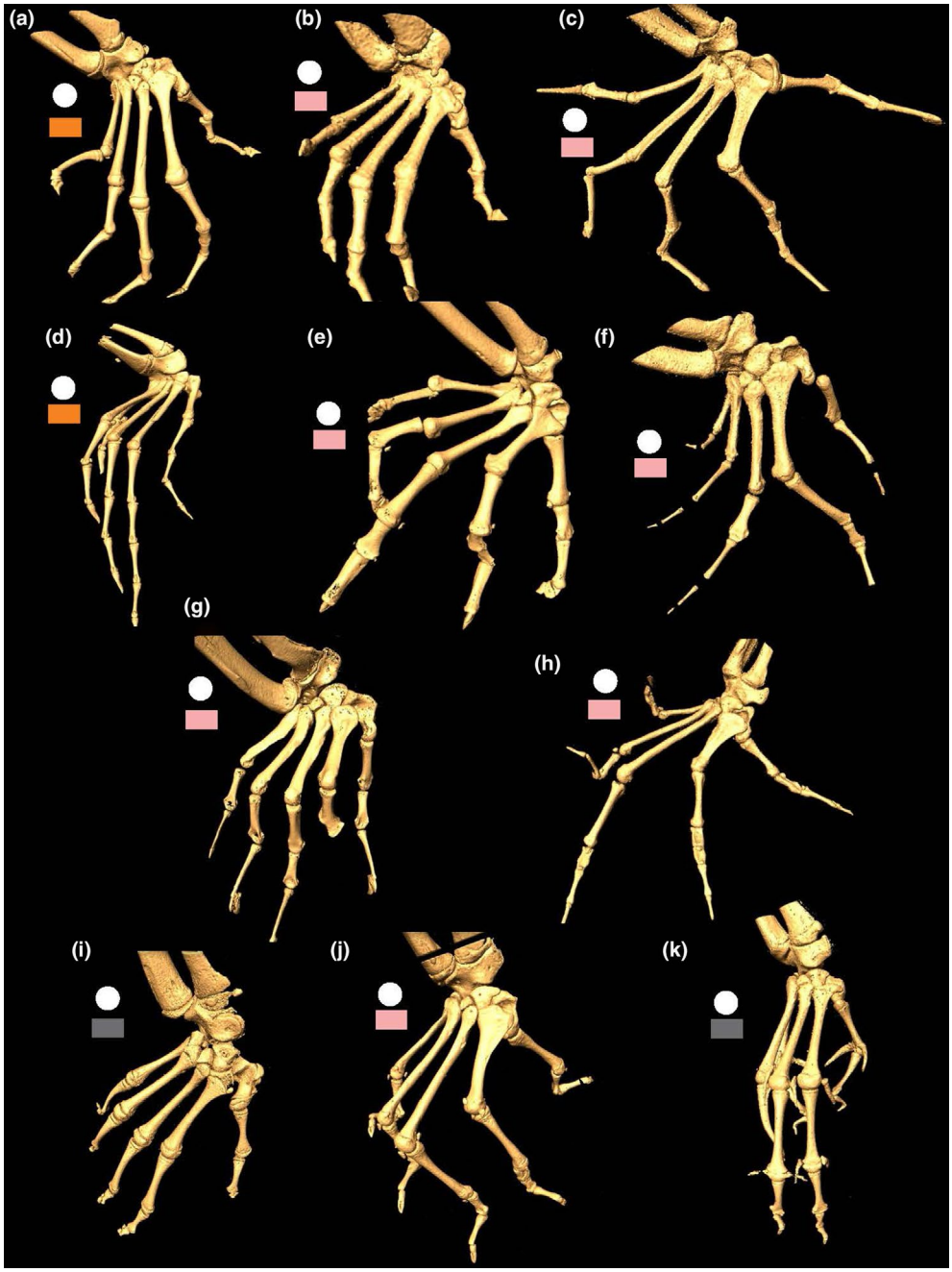

FIGURE 8 Micro-computed tomographic scan reconstructions of the lower crus and pedal regions of selected gekkotan lizards. All panels are of the left appendage; colored circles indicate family membership: White, Gekkonidae. Colored rectangles indicate toe pad condition: Orange, ancestrally padless; Pink, pad-bearing; Light grey, secondarily padless. Taxa in this figure belong to clade O depicted in figure 1 of Gamble et al. (2012)—see Table 1 for details. Species depicted are as follows: (a) *Nactus* sp., (b) *Dixonius siamensis*, (c) *Gekko kuhli*, (d) *Ptenopus* sp., (e) *Uroplatus lineatus*, (f) *Phelsuma* sp., (g) *Geckolepis* sp., (h) *Rhoptropus bradfieldi*, (i) *Chondrodactylus angulifer*, (j) *Pachydactlus punctatus*, (k) *Pachydactylus rangei*.

(Figures 9 and 10). The mesial border of the AC is gently rounded (Figures 9 and 10) and distally grades into a bulbous mesial tuberosity (Figures 9 and 10). An extensively developed meniscus intervenes between this tuberosity and MT I dorsally (Figures 3, 9, and 10) and abuts the proximal heads of MTs I–III and DT3 ventrally (Figure 10), thereby intruding into the structure of the tarsometatarsus in a manner similar to what might be expected of DT2 (were one present, as it is in *Sphenodon* Gray, 1831—Russell & Bauer, 2008).

The distal contours of the AC form an interlocking ridge and groove system with DT4 (Figures 9 and 10). A crucial part of this interlocking system is the large, sub-oval tarsal facet (Figure 9), a prominent feature on the dorsal and distal aspects of the AC. Distomesially, the element bears a pronounced rounded oblique ridge (Figures 9 and 10) that is bordered laterally by an oblique groove (Figure 10). Lateral to the groove, the contours of the AC become more pronounced. The groove grades into a broad,

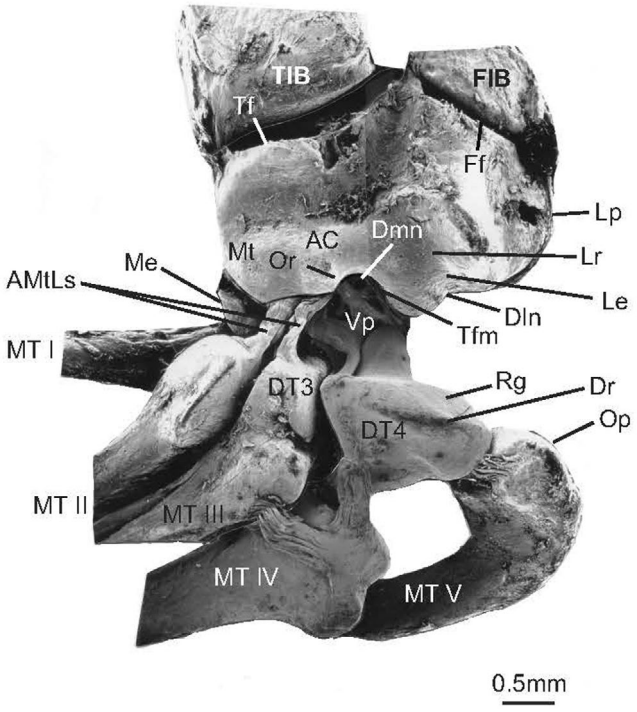

FIGURE 9 Scanning electron microscopic composite image of the dorsal aspect of a ligamentous preparation of the left ankle and tarsometatarsal region of *Anolis equestris*. Dr, dorsal ridge of the fourth distal tarsal. All other abbreviations as in Figures 2 and 3.

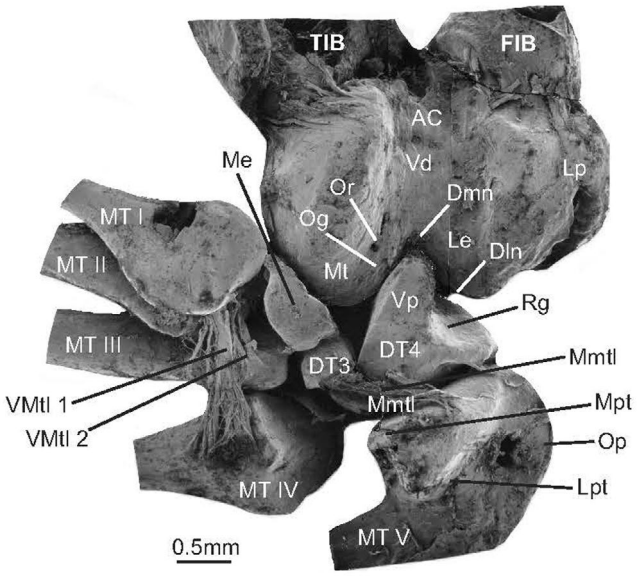

FIGURE 10 Scanning electron microscopic composite image of the ventral aspect of a ligamentous preparation of the right ankle and tarsometatarsal region of *Anolis garmani*. Og, oblique groove of the astragalocalcaneum; VMtl1, VMtl2, ventral intermetatarsal ligaments 1 and 2. All other abbreviations as in Figure 2.

oval, slightly convex lateral expansion (Figures 9 and 10) which is bordered by a thick margin of bone (Figures 9 and 10), the lateral rim (Figure 9), which is quite flat in *Anolis*. The oblique ridge and groove form the primary control surfaces of the mesotsarsal joint (Rewcastle, 1980), the lateral rim being a subsidiary surface (Rewcastle, 1980). The distomesial border of the tarsal facet bears a prominent distomesial notch (Figures 9 and 10), which is bordered mesially by the globular mesial tuberosity (Figures 9 and 10) and more laterally by the distally projecting oblique ridge (Figures 9 and 10). The distomesial notch receives the ventral peg of DT4 (Figures 9 and 10).

As in *Iguana* and *Pristidactylus* (Higham et al., 2021) the relative position of the distomesial notch of *Anolis* is such that its mesial margin is situated a considerable distance from the mesial border of the AC (Figures 2a and 9), rather than being situated very close to this border in *Gekko* (Figure 5; see also Higham et al., 2021, Figure 3a,b). Thus, the ventral peg of DT4 articulates with the AC approximately equidistant from the mesial and lateral borders of the latter in *Iguana*, *Pristidactylus* (Figure 2a) and *Anolis* (Figure 9), but is relatively more mesially located in *Gekko* (Figure 5a).

In *Anolis*, the distomesial notch of the AC is deep, and it is bordered by an oblique ridge that is pronounced and convex (Figures 9 and 10). The lateral process consists of a rounded and bulbous tubercle directed somewhat ventrolaterally and extends only slightly beyond the fibular facet (Figures 9 and 10). Functionally, the lateral process serves to maintain the positional relationships of the ventral cruropedal muscles that pass across this region to insert onto the plantar surface of the pes (Rewcastle, 1980) and it also provides the point of origin for muscles that adduct the pes relative to the crus.

Ventrally, the anoline AC is deeply indented (Figure 10). The ventral depression is broadest distally and gradually becomes narrower proximally (Figure 10). At the level of the tibial and fibular articulatory facets, this concavity expands slightly (Figure 10). Distally, this hollow is intruded into by the ventral peg of DT4 (Figure 10). The mesial aspect of the hollow is smooth, convex, and ovoid (Figure 10), with its proximodistal axis being the longest. While also offset from the ventral depression, the lateral edge is flatter and more rugose than the mesial surface (Figure 10). Along with the lateral process, the concave surface operates to prevent displacement of the ventral muscles (Rewcastle, 1980).

DT4 (Figures 9 and 10) is irregularly shaped and forms the distal part of the mesotarsal joint (Figures 9 and 10). Its broadest region is situated middorsally (Figure 9) and is sculpted laterally into a ventrolaterally to dorsomedially-trending ridge and groove (Figures 9 and 10), which separates a convex dorsal ridge (Figure 9) from the prominent rounded ventral peg (Figures 9 and 10) on the ventromesial corner. Thus, as in *Iguana* and *Pristidactylus* (Figure 2(a)) the ventral peg of DT4 of *Anolis* is offset mesially (Figure 9), whereas in *Gekko* it is somewhat more centrally situated (Higham et al., 2021, fig. 6a). The groove and ridge on DT4 (Figures 9 and 10) match reciprocal sculpturing on the AC (Figures 9 and 10). In *Anolis*, the ventral peg is narrow, elongate, and rounded (Figures 9 and 10).

In addition to articulating with the AC, DT4 also contacts MT IV and MT V distally (Figures 9 and 10) and DT3 mesially (Figures 9 and 10). The facet for MT V is ovoid, slightly concave, and located on the lateral margin of DT4 (Figures 9 and 10). It receives the subtly rounded mesial aspect of MT V (Figures 9–11). Articulation with

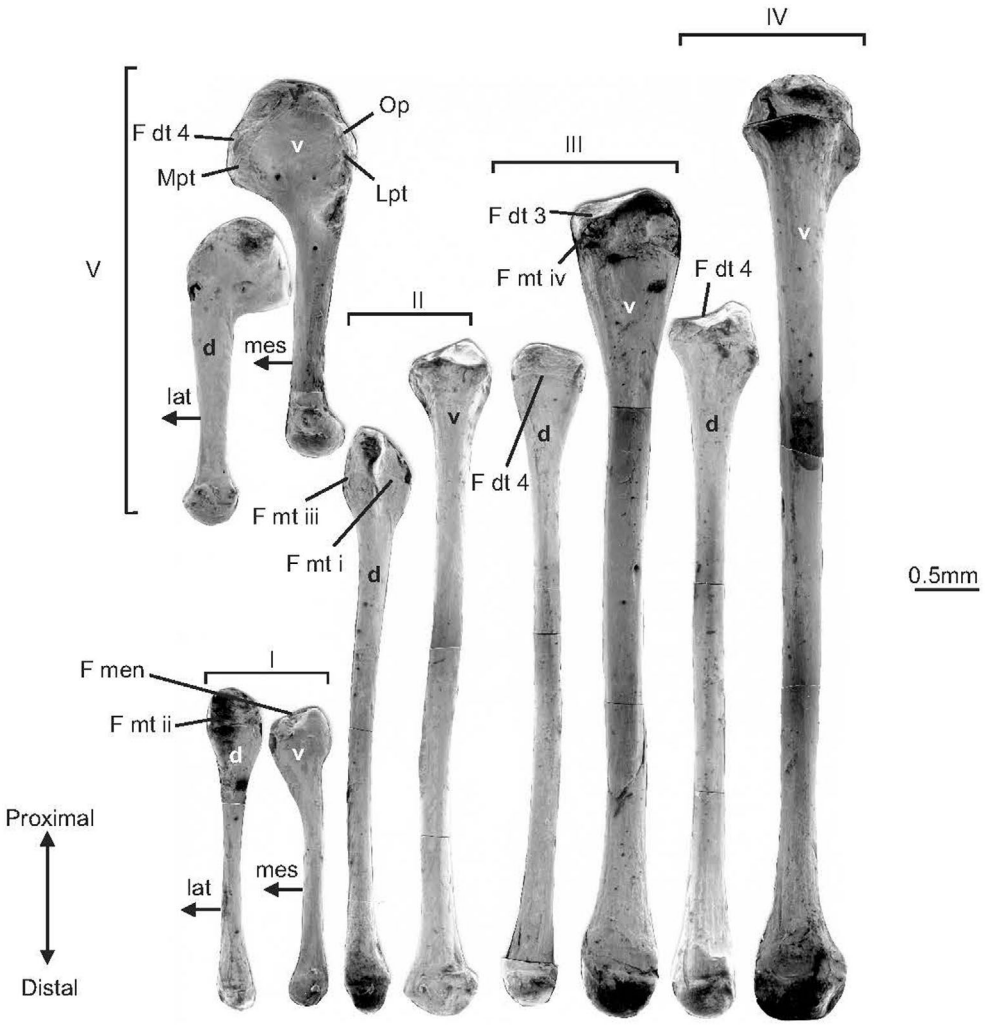

FIGURE 11 Scanning electron microscopic composite images of the metatarsals of the right pes of *Anolis garmani* in dorsal, d and ventral, v views. For each metatarsal pair (dorsal and ventral views) the two images are of elements from different individuals, hence their difference in absolute size. Metatarsals are numbered I–V, indicative of digital ray identity. Lateral and mesial aspects are indicated by "Lat" and "Mes," respectively. F men, facet for articulation with the meniscus; F mt i, F mt ii, facets for articulation with the first and second metatarsals, respectively. All other abbreviations as in Figures 2 and 6.

MT IV occurs via a poorly defined facet on the distal end of DT4 (Figure 9) that is positioned more dorsally than the facet for MT V (Figures 9 and 10). Articulation with DT3 is via a deep ovoid facet on the mesial margin of DT4 (Figures 9 and 10). The proximodistal axis of this facet is the longest and is surrounded by a rim of bone (Figure 9).

DT3 (Figures 3 and 9) is a small, rounded element that is bound to the proximomesial aspect of the head of MT III by a stout ligament (Figures 3 and 9). Its convex proximolateral aspect abuts a facet on DT4 (Figure 9). Mesially, it articulates with the meniscus (Figure 9). Dorsally, the proximal border of DT3 is attached to the AC via an astragalometatarsal ligament (Figures 3 and 9).

MT I (Figure 11) is the shortest metatarsal and has a bulbous proximal end. The lateral aspect of its proximal head abuts the adjacent meniscus (Figures 3, 9, and 10) which intervenes between it and the distomesial extremity of the AC. Ventrally, the proximal head of MT I is devoid of surface relief (Figure 11) and grades into a straight shaft that is smooth and ovoid in cross section, with a mesiolaterally trending long axis (Figure 11). Distally, the shaft expands into a unicondylar articulatory surface (Figure 11).

MT II is wedge-shaped proximally (Figures 9–11), its flat proximolateral margin abutting a similar planar surface on the proximomesial region of MT III (Figure 10). Proximally, MT II articulates with the meniscus (Figure 9) and mesially with the proximal head of MT I via a flat facet (Figures 9 and 11). The proximal head of MT II is slightly narrower ventrally than dorsally (Figures 9 and 10), thus the extent of imbrication is slight and largely involves MT I projecting ventral to MT II (Figure 10). The shaft of MT II, like that of MT I, is ovoid in cross section (Figure 11), with the long axis oriented mesiolaterally. In contrast to MT I, the shaft of the second curves slightly mesially (Figure 11). Similarly to the first, the distal end of the second is also unicondylar (Figure 11).

MT III (Figure 11) has a somewhat flattened, spade-shaped proximal end (Figures 10 and 11), the expanded surfaces of which

face ventrolaterally and dorsomesially (Figure 10). Besides being flatter than MT II, the third is also broader dorsally and ventrally (Figure 11). Overlap between MTs III and IV in *Anolis* is modest (Figures 9 and 10). Proximally, MT III articulates with DT3 for most of its width dorsally (Figures 9 and 10), but ventrally, articulation with the meniscus is extensive and takes place via a broad facet (Figures 10 and 11). The shaft is ovoid in cross section and is essentially straight. It terminates in a unicondylar distal articulatory surface (Figure 11).

MT IV (Figure 10) is shaped similarly to the third but is even more depressed (Figure 11). Proximally, the mesial aspect of its head bears a small diagonal facet for contact with MT III (Figure 11), while the lateral side is concave (Figure 11) for articulation with DT4. Compared to MT III, the distal end of MT IV is very expansive (Figure 11). Consistent with the other metatarsals, its distal articulatory surface is unicondylar (Figure 11).

The differential length pattern of the MTs of *Anolis* is generally similar to that of *Pristidactylus* (Table 1), but MT II is relatively much longer than MT I. The comparative lengths of MT II versus MT III and MT III versus MT IV are very similar in *Anolis* and *Pristidactylus* (Table 2). Comparison of the length of MT IV to MT I in *Anolis*, however, reveals a much greater differential than is evident for *Pristidactylus* (Table 2), indicative of an even more asymmetrical metatarsus. Compared to *Gekko gecko*, all differential comparisons of MT lengths (Table 2) are much greater for *Anolis* (see also Simoes et al., 2016 for further assessment of differential ratios between MTs in lizards).

MT V (Figures 10 and 11) has a hooked proximal end that is devoid of conspicuous contours. Ventrally, the mesial and lateral tubercles are not prominent (Figures 10 and 11), giving the plantar surface a relatively flat appearance (Figures 10 and 11). These tubercles lie far apart, with the mesial being positioned considerably more proximally than the lateral (Figures 10 and 11). The rounded proximolateral expansion is not pronounced (Figures 10 and 11). The shaft is relatively long and terminates in a distal unicondylar articulatory surface (Figures 10 and 11).

In accord with the morphology of the other MTs (Figure 11), MT V of *Anolis* has a relatively more elongate and gracile diaphysis than is evident in *Pristidactylus* (Figure 4) and its proximal, medially hooked end is less markedly sculpted, with less prominent mesial and lateral plantar tubercles, a shallower channel between them, and a more truncated outer process (Figures 4 and 11). Comparison of tubercle and process expression of MT V in *Anolis* (Figure 11) and *Gekko* (Figure 6) reveals that the outer process of the latter is much more massively built, the medial and lateral plantar tubercles are more prominent, and the channel between them is much deeper. The shaft of MT V is relatively much shorter and more robust in *Gekko* than it is in *Anolis* (Figures 6 and 11).

The synovial mesotarsal joint is enclosed by a fibrous capsule associated with a complex arrangement of intracapsular and extracapsular ligaments (Figures 3 and 12). The capsule consists of parallel and interlacing bundles of connective tissue fibers that enclose the joint and help to maintain the bony relations by restricting and guiding movements. Dorsally, the capsule is intimately involved in the epimysial sheaths of crural and pedal muscles passing near the region of articulation, these being the *m. peroneus brevis*, *m. extensor digitorum longus*, *m. tibialis anterior*, and the *m. extensores digitores breves* (Figure 13). Ventrally, the joint capsule is associated with an intricate, interconnected, layered network of tendinous sheets that comprise the plantar aponeurotic system (Russell, 1993) (Figure 13b,c). In *Anolis*, the *m. pronator profundus* contributes to the broad aponeurosis that adheres closely to the ventral surface of the AC (Figure 13d) and connects to the ovoid, fibrocartilaginous meniscus that intervenes between MTs I–III and the mesial tuberosity of the AC (Figures 3, 9, 10, and 12).

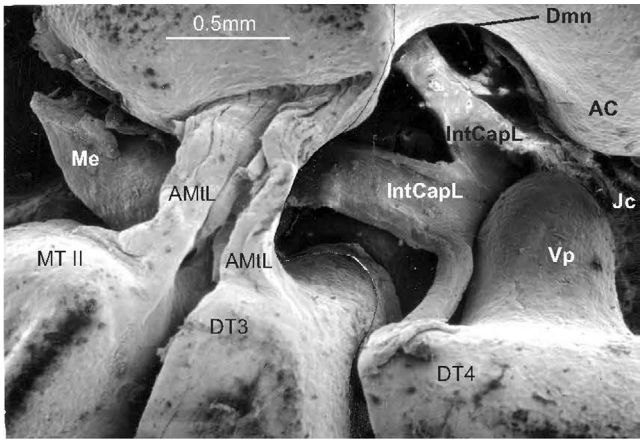

FIGURE 12 Scanning electron microscopic image of the ligaments of the ankle joint of the left pes of *Anolis equestris* in dorsal aspect. Jc, fibrous joint capsule. All other abbreviations are as in Figures 2 and 3.

The astragalometatarsal ligaments (Figures 3, 9, and 12) run between the distomesial aspect of the AC and the proximal ends of MTs I and II, and DT3. The astragalomeniscal ligaments (Figures 3 and 14) link the AC and the meniscus. Two emanate from the dorsomesial aspect of the AC, the first positioned proximal and lateral to the second (Figures 3 and 14). The first is thick and stout, forming a prominent band that passes obliquely across the AC before curving around its distomesial border (Figures 3 and 14). At the level of the mesial tuberosity of the AC this ligament becomes continuous with the meniscus. The second is considerably shorter (Figures 3 and 14) and flatter than the first and arises from the distomesial border of the AC, to which it adheres closely. At its proximal extremity, it is crossed by the first (Figures 3 and 14). Unlike the first ligament, the second is not continuous with the meniscus at the level of the mesial tuberosity (Figures 3 and 14), but instead joins it on its lateral border, deep to the astragalometatarsal ligaments (Figures 3 and 14). A third astragalomeniscal ligament, smaller than the other two, arises on the mesial border of the distomesial notch of the AC (Figure 14). It passes ventral to the astragalometatarsal ligaments to merge with the lateral border of the meniscus, along with the second astragalomeniscal ligament (Figure 14). In *Anolis*, the third astragalomeniscal ligament (Figure 14) is largely obscured by the stout astragalometatarsal ligaments.

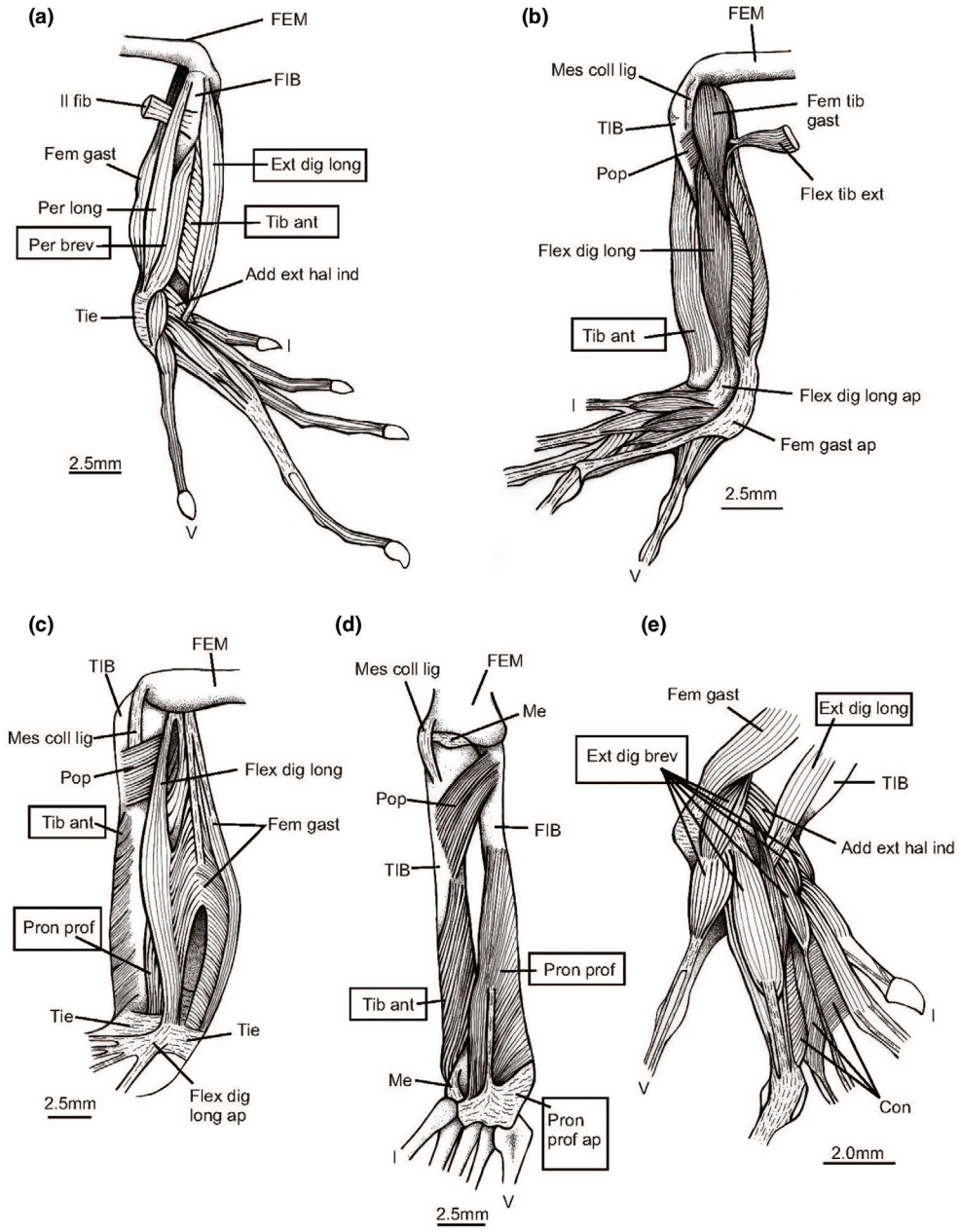

FIGURE 13 Muscles and associated aponeuroses of the right crus and pes of *Anolis garmani*. Those muscles having intimate contact, via aponeuroses or other tendinous structures, with the joint capsule of the ankle (mesotarsal) joint are indicated by black boxes surrounding the respective abbreviation. (a) Superficial extensor musculature of the crus. (b) Superficial flexor musculature of the crus after reflection of the *flexor tibialis externus* muscle. (c) Flexor musculature of the crus after removal of the femorotibial *gastrocnemius* muscle. (d) Deep flexor musculature of the crus after removal of the *flexor digitorum longus* and femoral *gastrocnemius* muscles. (e) Superficial extensor musculature of the distal region of the crus and the pes. Abbreviations (all muscle names follow the nomenclature of Russell & Bauer, 2008)—Add ext. hal ind, *m. adductor et extensor hallucis et indicus*; Con, *mm. contrahentes*; Ext dig brev, *mm. extensors digitores breves*; Ext dig long, *m. extensor digitorum longus*; FEM, femur; Fem gast, *m. femoral gastrocnemius*; Fem gast ap, aponeurosis of the *m. femoral gastrocnemius*; Fem tib gast, *m. femorotibial gastrocnemius*; FIB, fibula; Flex dig long, *m. flexor digitorum longus*; Flex dig long ap, aponeurosis of *the m. flexor digitorum longus*; Flex tib ext., *m. flexor tibialis externus*; Il fib, *m. iliofibularis*; Me, meniscus; Mes coll lig, mesial collateral ligament; Per brev, *m. peroneus brevis*; Per long, *m. peroneus longus*; Pop, *m. popliteus*; Pron prof, *m. pronator profundus*; Pron prof ap, aponeurosis of the *m. pronator profundus*; TIB, tibia; Tib ant, m. tibialis anterior; Tie, tie tendon; I, Digit I; V, Digit V.

The mesial tibioastragalar ligament (Figures 3 and 14) is closely associated with the astragalomeniscal ligaments and the meniscus. It is broad and arises from the distal aspect of the tibia, at the midpoint of the bone. It passes obliquely across the joint between the tibia and AC, tapering as it does so (Figures 3 and 14). Distally, it follows the mesial border of the AC and, at the level of the mesial tuberosity of the AC, merges with the first astragalomeniscal ligament and the meniscus (Figures 3 and 14).

The meniscometatarsal ligament (Figure 10) is extracapsular, emanating from the superficial surface of the meniscus, passing around the mesial margin of the AC, and coursing ventrally across the proximal end of the metatarsus to its attachment on the mesial plantar tubercle of MT V.

Dorsal intermetatarsal ligaments bind the first four MTs tightly together. Three ventral intermetatarsal ligaments run obliquely between the proximal heads of the first four MTs (Rewcastle, 1980, fig. 11b). Ventrally, a ventral intermetatarsal ligament arises from the proximolateral aspect of MT I and passes transversely across the plantar surface to attach to the proximomesial margin of MT IV (Figure 10). A second ventral intermetatarsal ligament arises from the proximolateral border of MT II and obliquely spans the interosseal gap between MTs II and III (Figure 10), attaching to the proximal region of the shaft of MT III. Similarly, a third ventral ligament spans the gap between MTs III and IV.

The intracapsular ligaments (Figures 12 and 14) have a complex branching structure. A ligament arises on the ventral surface of the AC, in the vicinity of the distomesial notch (Figure 12). At the level of the ventral peg of DT4, it joins two other ligaments, one that attaches to DT4 (Figures 10 and 14) and another that attaches to the meniscus (Figure 14). The ligament that extends dorsal to DT4 is slender, cord-like, and attaches to the mesial edge of the mesial ridge of this element (Figure 10). The other ligament, which becomes continuous with the meniscus, is broad. It emanates just mesial to the ventral peg of DT4, runs behind the astragalometatarsal ligaments, and attaches to the lateral border of the meniscus (Figures 10 and 14). In the region in which these ligaments intersect is a sheet of connective tissue that represents part of the fibrous capsule (Figure 12). This sheet passes proximal to the ventral peg of DT4.

4 | DISCUSSION

4.1 | Comparison of *Anolis* ankle and tarsometatarsal osteology and arthrology to that of *Iguana* and *Pristidactylus*

The pes of *Anolis* shares many morphological features with that of *Iguana* and *Pristidactylus*, particularly its marked asymmetry (Russell & Garner, 2023) (Figure 1b,d) and the general structure of the ankle joint and tarsometatarsus. There are, however, some notable differences. The most distinctive feature of the anoline AC, relative to its iguanian comparators, is its deeply hollowed ventral surface relative to the subtle concavity seen in *Iguana* and *Pristidactylus* (Figures 2b and 10). The orientation of the tibial and fibular facets also differs. In *Anolis*, the tibia and fibula abut more closely on the ventral surface than they do dorsally, while in the putatively ancestral condition (Higham et al., 2021; Rewcastle, 1980) they are equidistant dorsally and ventrally (Figures 2a,b, 9, and 10). The distomesial notch on the anoline AC is more pronounced than it is in *Iguana* and *Pristidactylus* (Figures 2a,b, 9, and 10), this being matched by a more distinct ventral peg on the fourth distal tarsal (Figures 2a,b, 9, and 10).

The contour of the tarsal facet on the AC is essentially consistent in all three taxa (Figures 2, 9, and 10). The ridges and grooves on the tarsal facet are matched in all by complementary structures on DT4 (Figures 2, 9, and 10). DT3 also differs little in form and anatomical relationships between these taxa. As such, key features of the mesotarsal joint are quite uniform, and they display relatively little morphological variation. This uniformity is concordant with the results of an extensive survey of lacertilian mesotarsal morphology conducted by Brinkman (1980). Except for varanids, the lateral process of the AC is very modestly extended from the body of this bone (Rewcastle, 1980), a configuration that is also exhibited by *Iguana*, *Pristidactylus*, and *Anolis* (Figures 2, 9, and 10).

In *Anolis*, the overall form of MTs I–IV is similar to that of *Iguana* and *Pristidactylus*, but the extent of imbrication between them is less (Figures 2a and 9); this being most evident in the minimal overlap of MT IV by MT III (Figures 9 and 10). This is a consequence of the head of MT IV exhibiting less apparent torsion (Rewcastle, 1980) of its shaft (Figures 4 and 11). In the putatively ancestral state (Russell & Bauer, 2008) the proximal head of MT II is overlapped laterally by DT3 (Figure 2a). In contrast, DT3 of *Anolis* does not overlie MT II and does not participate in the maintenance of the transverse arch (Figures 9 and 10). Compared to *Iguana* and *Pristidactylus* (Figure 4), the distal ends of all anoline MTs are unicondylar (Figure 11). MT V of *Anolis* (Figure 11) displays significant divergence from the pattern seen in *Iguana* and *Pristidactylus* (Figure 4), having a relatively longer shaft, a flatter ventral surface with much less surface relief, and a broadly expanded, unicondylar distal extremity. The first four MTs of *Anolis*, like those of *Iguana* and *Pristidactylus*, are subparallel in alignment (Figure 1d) and tightly bound by ligaments (Figures 2, 3, 9, 10, and 12).

The arthrology of the anoline pes is thus similar to that of *Iguana* and *Pristidactylus*, with all three displaying a complex mesotarsal joint bounded by a fibrous capsule that is attached to a system of ligaments and a meniscus (Figures 2, 3, 9, 10, and 12). Compared to *Iguana* and *Pristidactylus*, however, the meniscus of *Anolis* (Figures 9, 10, and 12) is relatively enlarged and ventrally supports the proximal extremities of MTs I–III (Figure 10), thereby providing an extensive gliding surface across the mesial tubercle of the AC. Laterally, the meniscus abuts DT3. These anatomical connections unify the bases of the first three digital rays.

External to the mesotarsal joint capsule are several ligaments that predominantly connect osseous elements on the mesial side of the pes, in the area between DT4 and MT I (Figures 2, 3, 9, and 10), a region in which the fibrous joint capsule is thickest.

DT4 is tightly bound by intracapsular structures (Figures 3, 12, and 14) and forms the major distal articular surface of the mesotarsal joint. As such, the intracapsular ligaments are crucial for maintaining alignment between the opposing ridge-and-groove features of DT4 and the AC. The ventral surface of DT4 is covered by the fibrous joint capsule, and an intracapsular ligament is bound to its dorsal

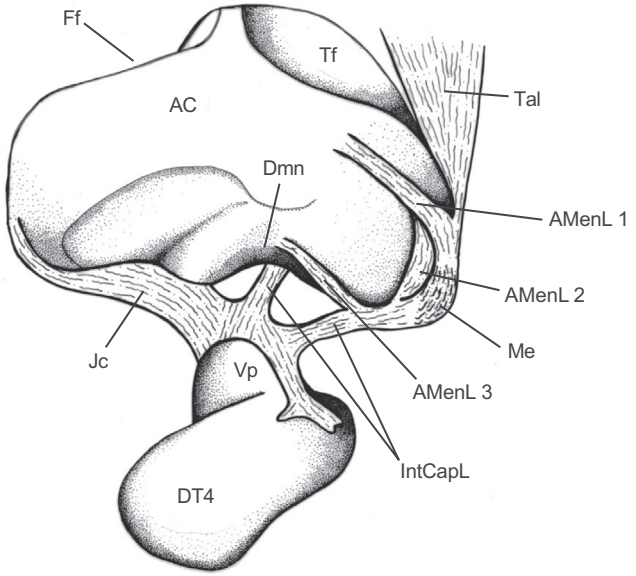

FIGURE 14 Schematic diagram of the fibrous joint capsule and intracapsular and extracapsular ligaments of lacertilians that govern the displacement of the fourth distal tarsal relative to the astragalocalcaneum. This rendition is a composite based upon the examination of numerous SEM photomicrographs representing several species. All abbreviations are as in Figures 2, 3 and 12.

ridge. Both the capsule and ligament operate in concert to control the displacement of DT4.

Besides being continuous with intracapsular ligaments, the meniscus is continuous with ligaments situated external to the joint capsule (Figures 2a, 3, and 14). Although these ligaments arise largely on the mesial aspect of the AC, some arise at a distance (Figure 14). These include the meniscometatarsal ligaments that link the ventral surface of the MTs to the meniscus (Figures 2b and 10), and the tibioastragalar ligament that arises on the distal end of the tibia (Figures 2a, 3, and 14).

While ligaments maintain the congruence between the articular surfaces of the mesotarsal joint, they also serve to tie the metatarsals together. MTs I–IV are tightly secured by both transverse and oblique ligaments (Figure 10), while the fifth diverges from the others and is not held tightly in place.

Features of MTs IV and V in *Anolis* contribute to enhanced digital mobility. The greater range of motion of digit IV of *Anolis* (Figure 1b,d) is related to the arrangement of the metatarsus and the structure of the metatarsophalangeal joint. Decreased imbrication of the metatarsus is associated with increased intermetatarsal flexibility (Robinson, 1975). All of the metatarsophalangeal joints of *Anolis* are unicondylar, providing greater freedom for lateromedial displacement (and possibly long axis rotation) of the digits than is possible in *Iguana* and *Pristidactylus*. The joint between MT IV and the first phalanx is further modified from the typical ginglymous pattern (Figure 11), with the bulbous, sub-hemispherical condyle of the former being received by a single, smaller reciprocal depression on the latter. The articulation between these two elements in *Anolis* permits a greater range of movement than is possible in *Iguana* and *Pristidactylus*. Similarly, the unicondylar distal head of MT V (Figure 11) is more broadly expanded than it is in *Iguana* and *Pristidactylus* (Figure 4). The relatively elongated shaft of the anoline MT V (Figure 11) increases the length of Digit V (Figure 1d), facilitating its role in grasping.

Limited information is available about the potential advantage of enhanced grasping ability of anoles in their structural habitat, although behavior in extreme weather events has shone some light on this (DiPaolo & Kolbe, 2023; Donihue et al., 2018). Robinson (1975) illustrated two postures adopted by *Anolis equestris* on tree branches in an artificial setting. In the first, the crus is flexed and Digit V opposes the other four in a clasp grip around a branch. In a second posture, the crus is extended, and Digit V is hooked over the top of the branch, with the other four digits not participating in the clasp. In a behavioral study of *Anolis lineatopus* Gray, 1840 in Jamaica, Rand (1967) found that it rests on narrow branches, with its hind legs either flexed or extended, as depicted by Robinson (1975). According to Rand (1967), the grasp on the branch is so strong that grip is maintained even during violent shaking of the perch. In his assessment, however, Rand (1967) did not distinguish between attachment due to mechanical grasping and that which might be attributable to adhesive contact (DiPaolo & Kolbe, 2023). In *Anolis*, interspecific differences exist in the posture adopted when resting on a perch (Rand, 1967), and in the selection of perch diameter when sprinting and jumping (Moermond, 1979; Schoener & Schoener, 1971). The selection of perch diameter has been related to morphological dimensions such as hind limb length (Losos & Irschick, 1996; Losos & Sinervo, 1989; Pounds, 1988), but the relationship between digital morphology, grasping ability, and perch preference in the different ecomorphs remains uninvestigated. Buettell and Losos (1999) examined the lengths of distal limb elements in different anole ecomorphs but did not consider the locomotor implications of these measurements in terms of digital movement.

Abdala et al. (2014) noted that *Anolis* can grasp narrow branches by wrapping its digits around them, but found no defining anatomical features associated with this ability when compared to other iguanian lizards (*Diplolaemus* Bell, 1843, *Enyalius* Wagler, 1830, *Iguana* Laurenti, 1768, *Liolaemus* Wiegmann 1834, *Leiosaurus* A.M.C. Duméril & Bibron, 1837, *Phymaturus* Gravenhorst, 1838, *Polychrus* Cuvier, 1817 and *Tropidurus* Wied-Neuwied, 1824). This versatility of function was instead attributed to behavioral differences (Abdala et al., 2014), but it is noteworthy that the data upon which these conclusions were based were restricted to lengths of skeletal elements alone (femur, tibia, metatarsals, and phalanges), omitting any consideration of their anatomical form and relationships, and eschewing entirely any consideration of the tarsals. The aforementioned modified metatarsophalangeal joints of *Anolis*, however, are likely contributory to the enhanced grasping capabilities noted for this taxon.

4.2 | Comparison of ankle and tarsometatarsal osteology and arthrology of *Anolis* and geckos

The tarsometatarsus of *Gekko gecko* (Figure 6) and other geckos (Figures 7 and 8) exhibits extensive modifications related to

pronounced digital spreading (Figure 1c) as well as the propensity for abduction/adduction of the entire tarsometatarsus relative to the long axis of the crus. The contact of DT4 with MT V is much more robust in *Gekko* than it is in *Anolis*. DT4 of *Anolis* is relatively much broader distally than that of *Gekko*, and contact with MT IV is much more restricted. MT V of *Gekko* is relatively much more robust than that of *Anolis* (and other iguanians), and has a very prominent and proximolaterally-projecting outer process that provides insertion for components of the *m. abductor digiti quinti* (Russell & Bauer, 2008) originating from the flange-like lateral process of the AC. MT V of *Anolis* has a long and slender shaft, relatively longer than that of its iguanian comparators (*Iguana* and *Pristidactylus*), and thus contrasts greatly with that of *Gekko* (and most other geckos—Figures 7 and 8) in which the length of the shaft is markedly truncated. Indeed, whereas the entire metatarsus of *Gekko* (and other geckos, in general) exhibits relative truncation of its entire length (Russell et al., 1997; Simoes et al., 2016), that of *Anolis* (Figure 11) is relatively elongated compared to its iguanian comparators (*Iguana* and *Pristidactylus*—Figure 4) and non-gekkotan lizards in general (Russell et al., 1997 provide comparative information for *Anolis carolinensis* Voigt, 1832, *Iguana iguana*, *Sceloporus undulatus* (Bosc & Daudin, 1801), *Uta stansburiana* Baird & Girard, 1852, *Agama* Daudin, 1802 sp., *Pogona barbata* (Cuvier, 1829), *Caledoniscincus austrocaledonicus* (Bavay, 1869), *Marmorosphax tricolor* (Bavay, 1869), and *Sigaloseps deplanchei* (Bavay, 1869)).

The entire digital array of *Gekko* can be displaced laterally because the unified tarsometatarsus can pivot about the semicircular distomesial notch of the AC (Higham et al., 2021). In *Gekko* there is direct contact of MT IV with MT V, thus DT4, MT IV, and MT V are united as a unitary lever. DT3 connects with this complex more medially via its extensive contact with DT4, and the broad abutment of the proximal end of DT3 with DT4 brings the more medial MTs (I and II) into this integrated articulatory pattern. The proximal heads of MTs I–IV imbricate less (Simoes et al., 2016) than they do in *Anolis* (and other lizards in general). These features provide the pes of *Gekko* (and geckos in general—see Figures 7 and 8) with remarkable capacities of adduction and abduction of the entire pes relative to the long axis of the crus (Figure 1c). This is augmented by the ability to adduct or abduct the digital rays relative to each other, as per the vanes of a fan (Figure 1c). These coordinated actions enable the adhesive toe pads to be deployed in configurations that can optimize their loading patterns regardless of body orientation, enabling the adhesive system to respond to variations in body orientation (Russell & Oetelaar, 2016; Song et al., 2020). Geckos are thus able to alter digit positioning during locomotion or static clinging (Higham et al., 2021), thereby effecting "adjustable distributed control" (Song et al., 2020) of the adhesive apparatus. Adjustment of digit orientation is thus not limited to movement of the digital rays solely at the metatarsophalangeal joints. In *Anolis* much of the displacement of the digits relative to one another occurs at the metatarsophalangeal joints (Figures 1b,d and 11), although digits I–III are united by their collective association with the large meniscus that intervenes between them and the mesial tubercle of the AC (Figure 10). As in non-gekkotan lizards in general (those with unreduced limbs or digits), the pes of *Anolis* rolls onto its mesial border at the end of the stance phase (Brinkman, 1980; Rewcastle, 1980, 1981; Robinson, 1975) via pedal plantarflexion and conjoint rotation at the ankle joint (Russell & Bels, 2001), resulting in contact with the substratum along the metatarsophalangeal line (Russell & Bauer, 2008, fig. 1.19), with Digits V and IV losing contact with the substratum early (Rewcastle, 1981; Russell & Bels, 2001), prior to continuance of pedal plantarflexion and ultimate release of the more mesial toe pads (Russell & Bels, 2001) of Digits II and III (Digit I is devoid of a definitive toe pad—Figure 1d). The unification of digital rays I–III in *Anolis*, via the means described above, provides stability to this sector of the tarsometatarsus. The progressively less restrictive articulations between the metatarsals and the proximalmost phalanges of each digit (Figure 11), from Digit I–V, provide the more laterally situated digits (especially IV and V) with greater possibility for mediolateral displacement (Figure 1d) and long-axis rotation than the more medial ones.

DT4 of *Gekko* diverges markedly from the morphology of the ancestral lacertilian form (Robinson, 1975). In lizards in general, DT4 is an ovoid element that articulates loosely with the adjacent DT3 and MTs IV and V via shallow facets (Rewcastle, 1980). This morphology is clearly evident in *Anolis* (Figures 9 and 10), closely resembling the pattern found in *Iguana* and *Pristidactylus* (Figure 2). Relative to the ancestral pattern, the lateral articulatory facet on the gekkonid DT3 for receipt of DT4 is better defined. DT4 of *Gekko* is relatively much more elongated proximodistally while being narrower mediolaterally. Its ventral peg is relatively very small (Higham et al., 2021, fig. 6a), contrasting markedly with the prominent ventral peg of *Anolis* (Figure 9) that is of relatively greater size compared to that of *Iguana* and *Pristidactylus* (Figure 2a). The ventral peg of DT4 of *Gekko* is sufficiently small that it does not restrict displacement of DT4 on the distal articulatory surface of the AC (Higham et al., 2021, figs 4, 6), allowing for mediolateral translation of DT4 (and thus the pes) independent of pedal long axis rotation or pedal plantarflexion. The articulatory surface between the AC and DT4 that constitutes the ankle joint is, in a relative sense, more medially situated in *Gekko* (Figure 5a) than it is in *Iguana*, *Pristidactylus* (Figure 2a,b), *Anolis* (Figures 9 and 10) and other lizards (Rewcastle, 1980), this being due to both its proximity to the medial border of the AC and because of the extensive lateral process of the AC (Figure 5a). This relatively more medial positioning of the ankle joint, along with the less constrained patterns of movement it allows (Higham et al., 2021), provides a longer lever arm for the action of the *m. abductor digiti quinti* (Russell & Bauer, 2008) that spans from that process to the ventral aspect of MTV. In contrast, the relatively more lateral positioning of the mesotarsal joint and the relatively small lateral process of the AC of *Anolis* (Figures 9 and 10) indicate that motility at the mesotarsal joint is more restricted, in a similar fashion to that of non-gekkotan lizards in general (Rewcastle, 1980). As noted above, the most distinctive feature of the anoline AC, relative to its iguanian comparators, is its deeply hollowed ventral surface relative to the

subtle concavity seen in *Iguana* and *Pristidactylus* (Figures 2b and 10). This is associated with the relatively large ventral peg on DT4 of *Anolis*, and its accommodation within the deep depression on the ventral surface of the AC (Figure 10), the latter being flanked by a very prominent medial tubercle and a steeper-walled lateral expansion. Displacement possibilities of DT4 on the AC in *Anolis* are similar to those for non-gekkotan lizards (Rewcastle, 1980) and ensure conjoint long axis rotation and flexion/extension of the pes at the mesotarsal articulation.

The widely radiating digits of the pes of *Gekko gecko* (Russell, 1975; Russell et al., 1997) (Figure 1c) contrast markedly with the anoline pattern (Figure 1d). This secondary symmetry is a ubiquitous feature of gekkotans, even ancestrally padless forms (Figures 7 and 8; Russell et al., 1997) and is exaggerated in pad-bearing gekkotans (Figures 5, 7, and 8). Digits III and IV, and II and V are subequal in length (Figure 1c), and the MT rays are widely divergent. The broadly expanded head of MT IV (Figure 6) greatly increases the angle between the shafts of MTs III and V (Russell et al., 1997). As a result, the toe pads are able to be accommodated in the interstices between the digits and to be disposed in parallel across the pes (Russell & Garner, 2023; Zhuang et al., 2019) (Figure 1c), rather than being staggered from digit to digit as is the case for *Anolis* (Russell & Garner, 2023) (Figure 1d).

The morphology of MT V is regarded as being highly informative about locomotor mechanics. In squamates, it is a morphologically complex bone (Robinson, 1975) that ventrally bears tubercles and an expanded outer process for the attachment of muscles, including the *m. femoral gastrocnemius* and the *m. peroneus* complex (Robinson, 1975) (Figure 13). Its plethora of variable features makes it one of the most informative of postcranial bones of diapsid reptiles (Borsuk-Białynicka, 2018). Rothier et al. (2017) advocated that Digit V, inclusive of its MT, is of particular and peculiar importance to locomotor performance in lizards. MT V increases the leverage of the pedal flexors (Brinkman, 1980; Robinson, 1975), this role being independent of the phalanges of Digit V. Russell and Rewcastle (1979) examined the morphology of MT V of *Sitana* Cuvier, 1829, an agamid that is bipedal at high speeds and exhibits loss of the phalanges of Digit V. Although the shaft of MT V is absent in *Sitana*, its proximal portion is not modified, with tubercles and the lateral process retaining their form and muscular associations. Rothier et al. (2017) found that non-climbing geckos have a longer MT V than climbers (that is, geckos with adhesive toe pads). Such findings contrast with *Anolis*, which exhibits relatively elongated MTs (Figure 11; Table 2), including MT V, and digits compared to *Iguana* and *Pristidactylus* (Figure 4), and much longer digits when compared to pad-bearing geckos (Figure 1c,d). The secondarily symmetrical morphology of the pes in pad-bearing geckos has converged upon the architectural arrangement of the lacertilian manus.

The asymmetrical form of the pes of *Anolis* (Figure 1d) is similar to that of normal-limbed lizards in general. Some geckos exhibit trends toward secondary asymmetry of the pes in association with particular habitat associations. The gekkonid genus *Phelsuma* Gray, 1825 is regarded as being ecologically similar to *Anolis* (Wright et al., 2021). Pedal form in *Phelsuma* has been linked to arboreality (Russell et al., 1997; Zhuang & Higham, 2016) and provides insight into the deployment of the asymmetrical foot of *Anolis* in similar ecological circumstances. The reduction in size of pedal Digit I of *Phelsuma*, the absence of a toe pad on this digit, elongation of Digit IV, and the large angle between Digits IV and V likely assist grasping of branches between the more medial digits and the fifth. High-speed video has revealed that *Phelsuma* uses its elongated fourth digit to facilitate wrapping its foot around small branches while running (Zhuang & Higham, 2016), a posture noted by Robinson (1975) for *Anolis* when grasping branches. Asymmetry may also facilitate propulsion on relatively broad arboreal surfaces, such as tree trunks, by increasing the number of distal metatarsal tips (I–III aligned to form the metatarsophalangeal line) involved in propulsion (Rewcastle, 1981, 1983). For *Anolis*, these factors might help explain the persistence of pedal asymmetry, digital elongation, and its strong association with arboreal habitats. Rather than exhibiting a metatarsus with proportional lengths similar to those exhibited by *Gekko* (Figure 6) and other geckos (Figures 7 and 8), *Anolis* exhibits the opposite trend in comparison to *Pristidactylus*, with the length differentials being increased (Table 2). Additionally, the first four MTs of *Anolis* (Figure 9) are visually more gracile than those of *Pristidactylus* (Figure 4) and considerably less robust than those of *Gekko* (Figure 6). The relative increase in the length of the pes of *Anolis*, achieved through its elongated MTs (Table 2) and long digits, and the gracility of these skeletal elements possibly assist in sprinting (Irschick & Losos, 1998) and proficiency in jumping (Bels et al., 1992; Gillis et al., 2009; Toro et al., 2003, 2004), a behavior frequently employed when traversing tight turns while sprinting along perches (Higham et al., 2001).

Digit V of the pes of lizards is capable of marked divergence from the long axis of the pes (Figure 1d), and upon flexion, can oppose Digit I (Robinson, 1975). Digit IV is also capable of marked abduction/adduction (Figure 1d) and can complement digit V by producing flexion opposition to the first three digits, this being most marked in arboreal forms such as anolines (Rewcastle, 1981, 1983). Brinkman (1980) found that in *Anolis*, flexion of Digit V can bring its plantar surface into opposition with the other digits, with no long axis rotation of Digit V being required, in contrast to *Iguana*. Such attributes are associated with the ability of *Anolis* to grasp perches of relatively narrow diameter when resting, running, and jumping (Gillis et al., 2009; Higham et al., 2001; Toro et al., 2003, 2004).

As shown by Brinkman (1980), the ligamentous features of the mesotarsal joint are similar in a variety of taxa, including *Anolis* and *Gekko gecko*. Both taxa share with *Iguana* and *Pristidactylus* a complex arthrology of the mesotarsal joint that internally involves a fibrous capsule attached to a system of ligaments and a meniscus, as well as extracapsular ligaments (Figures 2, 3, 5, 9, 10, 12, and 14). Transverse and oblique intermetatarsal ligaments in *Gekko gecko* (Russell, 1975, fig. 10a) accord with those described for *Anolis*. Thus, the connective tissue structures that ultimately govern displacements at the ankle joint and within the tarsometatarsus do not differ in number or general anatomical relationships (Figures 2, 3, 5, 9, 10, 12, and 14), but their courses and extent are altered in accordance

with changes in the form of the skeletal elements and muscles with which they are associated.

4.3 | Potential implications of morphological differences for gecko and *Anolis* locomotion

Our anatomical findings relating to pedal osteology and arthrology of *Anolis* and geckos provide baseline qualitative information for further exploration of locomotor mechanics and how these relate to the deployment of a digitally located adhesive system in these two clades. Given the evidence available to us so far, we point out some promising areas for future investigation, identifying predictions and hypotheses that will benefit from appropriately designed comparative observations.

Overall the structure of the ankle joint and tarsometatarsus of *Anolis* is much more similar to that of lizards in general (Rewcastle, 1980), and to the iguanian comparator taxa (*Iguana* and *Pristidactylus*) employed in this study, than it is to *Gekko* (and gekkotans in general—Russell et al., 1997; Figures 7 and 8). The osteology of the ankle joint and tarsometatarsus of *Anolis* (Figures 9–11) differs considerably from that of *Gekko gecko* (Figures 5 and 6) or geckos in general (Figures 7 and 8). The most obvious differences between the two are that the pes of *Anolis*, like that of other non-gekkotan taxa, is markedly asymmetrical (Russell et al., 1997; Russell & Garner, 2023) and its MTs are relatively greatly elongated (compared to the iguanian comparators examined herein). The distal tips of the first three MTs of *Anolis* lie on a straight, oblique line (Rewcastle, 1980, 1981). The arrangement of the anoline metatarsus has implications for the location of the subdigital adhesive pads as it limits their spatial disposition (Russell & Garner, 2023). On the widely spaced digits of the manus of *Anolis*, digits three and four are subequal in length, and the pads are aligned adjacent to one another (Russell & Garner, 2023). On the pes, however, where the MTs are configured with their long axes more or less in parallel (Figure 1d), the greatly discrepant length of the digits mitigates against the pads otherwise encroaching on one another (Russell et al., 1997) by staggering them.

Although adhesive toe pads are a feature of both anoles and geckos, they have been incorporated into the structure of the pes in different ways. The findings of Hagey, Harte, et al. (2017) that led them to the conclusion, following comparison of limb, and limb segment, lengths of anoles and geckos, that "there is more than one way to climb a tree" are thus associated not only with the expression of different limb length proportions but also with differences in skeletal configurations that determine limb actions. As Dang et al. (2018) point out, skeletal morphology is related to the ways in which habitat characteristics are exploited by the locomotor system. Lizards can exhibit a surprising amount of variation in skeletal elements that reflect differences in joint conformation (Regnault et al., 2016). Joint structure, and the osteology of limbs, determine kinematic patterns and their details can reveal a great deal about how different taxa exploit the locomotor environment, even though such an environment might appear to impose the same selective forces upon all taxa employing it.

Given the anatomical differences that are evident, we predict that the great versatility of displacement of the pes of *Gekko* (Higham et al., 2021) and other geckos (Russell & Oetelaar, 2016) is not achievable by *Anolis*. Body orientations that can be achieved during static clinging and the agility displayed during locomotion on smooth substrata when the setal adhesive system serves as the sole means of contact and attachment will be constrained in anoles when compared to geckos. Studies similar to that conducted by Russell and Oetelaar (2016) will be informative in the assessment of the range of pedal postures and toe pad orientations achievable by anoles, and how these relate to the osteological and arthrological attributes of the hind foot.

Available comparative information provides support for the above-mentioned prediction. Wright et al. (2021) found that the gecko *Phelsuma laticauda* (Boettger, 1880) used smooth perches more frequently than either *Anolis carolinensis* or *A. sagrei* Duméril & Bibron, 1837 in an enclosure experiment in Hawaii. Differences in the morphology of the ankle joint between geckos and anoles may be associated with these differences in surface use. Although geckos and anoles have been shown to generate static clinging forces of similar magnitude when corrected for body size and mass (Garner et al., 2021; Irschick et al., 1996; Wright et al., 2021), static clinging performance and locomotor versatility are not necessarily directly related (Higham & Russell, 2025; Russell & Gamble, 2019). The relative ease with which geckos traverse smooth vertical surfaces in all directions (Song et al., 2020) is not exhibited by anoles, indicating that the mechanics involved with rapid locomotion in such circumstances are not equivalent in these two lineages. As Clark and O'Connor (2021) note, responses to the same general selective pressures may result in functionally similar outcomes that may be anatomically dissimilar (and, thus, mechanically different), reflective of many-to-one mapping of form to function (Wainwright et al., 2005), in which complex systems promote the evolution of diversity. Ecomorphological and ecomechanical studies that incorporate knowledge of internal and external anatomical features in relation to habitat use will assist in furthering our understanding of how the digital adhesive system is integrated into the locomotor repertoire of anoles and geckos. Future studies should consider such factors when exploring the relationships between morphology, mechanics, and ecology of geckos and anoles.

Ankle morphology may also reflect the types of perches/substrates exploited in nature. Several studies have quantified the locomotor kinematics of *Anolis* running on cylindrical perches (e.g., Foster & Higham, 2012; Losos & Sinervo, 1989), these being akin to substrata commonly exploited by these lizards in their arboreal habitats (Mattingly & Jayne, 2004). It appears that geckos use narrow perches less frequently. To date, only a single study has examined gecko locomotion on narrow perches (Zhuang & Higham, 2016). That study found that *Phelsuma madagascariensis* Gray, 1831 increases long-axis humeral rotation and decreases femoral rotation with decreasing perch diameter. This is similar to responses

recorded for *Anolis carolinensis* (Foster & Higham, 2012), suggesting similar accommodations to changes in perch diameter. Zhuang and Higham (2016) discovered, however, that the ankle is increasingly flexed throughout the stance phase of the stride on narrow vertical perches in *Phelsuma* (culminating in an angle of approximately 50°), whereas Foster and Higham (2012) found that the ankle of *A. carolinensis* undergoes a flexion-extension motion throughout stance under the same conditions, culminating in an ankle angle of approximately 140°. Zaaf et al. (2001) documented differences in ankle kinematics between *Gekko* and non-gekkotan lizards, also noting the lack of extension during the propulsive phase of stance. The lack of extension during the propulsive phase of stance in *Phelsuma* (Zhuang & Higham, 2016) suggests that the ankle is less suited to propulsion on narrow perches in geckos than it is in anoles. We predict that the morphological configuration of the ankle of *Anolis* is more efficient than that of geckos in facilitating the propulsive phase on narrow perches. Future comparative work should focus on ankle and foot morphology in relation to the facility of movement in different types of habitats.

The cadence of digit detachment differs between pad-bearing geckos and *Anolis*, the former employing active hyperextension of the digits, from tip to base, prior to the commencement of pedal plantarflexion (Russell & Higham, 2009), whereas *Anolis* employs pedal plantarflexion to release its toe pads, hyperextension of the latter resulting from the digits detaching from base to tip (Garner et al., 2021; Russell & Bels, 2001). Although the release sequence of the digits is unchanged from that in non-gekkotan lizards (Digit V releases first, followed by IV, then III, then II+I; Russell, 2002), geckos employing active digital hyperextension have modified muscles in the digits (both manus and pes) that contract prior to pedal plantarflexion (and its equivalent in the manus). The symmetrical, fan-like disposition of the digits (Figure 1c) is associated with this change in digital release pattern (Russell, 2002). We hypothesize that the marked asymmetry of the pes, and the staggered disposition of the toe pads in adjacent digits of *Anolis* (Russell & Garner, 2023) (Figure 1d) mitigate against the operation of active toe pad hyperextension.

Given that the predicted relatively low level of similarity of anatomical detail of ankle and tarsometatarsus structure of *Gekko* and *Anolis* was corroborated, we recognize that a more extensive comparison with geckos is necessary. Geckos encompass six families of lizards whereas *Anolis* is a single genus. Among geckos, there have been multiple origins of the adhesive system (Gamble et al., 2012; Russell & Gamble, 2019), but only a single origin in the Anolidae (Losos, 2009; Russell & Garner, 2023). Some gekkotan taxa exhibit some ankle and tarsometatarsal features that are more similar to those of non-gekkotan lizards (Higham et al., 2021; Russell et al., 1997; Russell & Bauer, 2008) than are those of *Gekko*, even though they retain most of the characteristics of the suite of osteological attributes of geckos in general. Such patterns are associated with both ancestrally padless (Figure 7b) and possibly secondarily padless (Figure 8d) (Russell & Gamble, 2019) psammophilous terrestrial species. Zhuang et al. (2019) found that reduction and loss of the adhesive system in geckos may lead to the regaining of morphological attributes of pedal structure similar to those of ancestrally padless lineages. Geckos are not invariant in the configuration of the pes and much remains to be explored about the specializations that they show in relation to particular habitats and the challenges imposed by different substrata. Furthermore, those geckos with incipient adhesively competent toe pads, such as *Gonatodes humeralis* (Guichenot, 1855) (Higham et al., 2017; Russell et al., 2015), that, similarly to *Anolis* (Russell & Bels, 2001), employ passive hyperextension of the adhesive structures, may exhibit ankle joint and tarsometatarsal structure more akin to that of *Anolis*. Descriptions of the tarsal and metatarsal elements of *Gonatodes humeralis* furnished by Rivero-Blanco (1976) do not provide sufficient detail to enable evaluation of this possibility. More detailed analysis of pertinent anatomical structure in these, and other promising candidate taxa with incipient toe pads (Russell & Garner, 2023) is required.

Anoles and geckos have acquired adhesive toe pads and incorporated them into their locomotor repertoires from structurally different starting points. The pes of geckos departed far from the ancestral structural pattern of lizards early in the phylogenetic history of this clade (Russell et al., 1997; Russell & Gamble, 2019; Simoes et al., 2016). Toe pads were incorporated into a configuration quite different from that of the ancestral lacertilian pattern (Evans, 2003; Rewcastle, 1980, 1981, 1983; Robinson, 1975). In contrast, anoles have amalgamated the acquisition and operation of toe pads into a morphological pedal framework that is much more similar to the ancestral lacertilian pattern (Russell & Garner, 2023), although it does exhibit its own specializations. Thus, possession of adhesive toe pads in geckos and anoles, while dependent upon the same physical principles for attachment (Russell & Garner, 2023), has been coopted into pedal architecture that is configured quite differently.

AUTHOR CONTRIBUTIONS

Concept design: APR and TEH. Data acquisition: LDM and APR. Data analysis and interpretation: APR, LDM, and TEH. Drafting of the manuscript: APR, LDM, and TEH. Critical revision of the manuscript: APR and TEH. Approval of the article: APR and TEH.

ACKNOWLEDGMENTS

We thank Philip Bergmann for assistance with radiography, Heather Jamniczky, and Minga Zhuang for assistance with the CT scanning, and the staff of the Microscopy and Imaging Facility, Cumming School of Medicine, University of Calgary for assistance with scanning electron microscopy. We thank Lee Grismer (Figure 1a) and Colin Donihue (Figure 1d) for granting us permission to include their photographs.

FUNDING INFORMATION

This study was supported by an NSERC Discovery Grant (A9745-2008) to APR.

CONFLICT OF INTEREST STATEMENT

The authors declare that they have no conflicts of interest.

DATA AVAILABILITY STATEMENT

Data sharing not applicable to this article as no datasets were generated or analysed during the current study.

ORCID

Anthony P. Russell https://orcid.org/0000-0001-6659-6765
Timothy E. Higham https://orcid.org/0000-0003-3538-6671

REFERENCES

Abdala, V., Tulli, M.J., Russell, A.P., Powell, G.L. & Cruz, F.B. (2014) Anatomy of the crus and pes of neotropical iguanian lizards in relation to habitat use and digitally based grasping capabilities. *The Anatomical Record*, 297, 397–409.

Autumn, K. & Peattie, A.M. (2002) Mechanisms of adhesion in geckos. *Integrative and Comparative Biology*, 42, 1081–1090.

Autumn, K., Sitti, M., Liang, Y.A., Peattie, A.M., Hansen, W.R., Sponberg, S. et al. (2002) Evidence for van der Waals adhesion in gecko setae. *Proceedings of the National Academy of Sciences of the United States of America*, 99, 12252–12256.

Bels, V.L., Theys, J., Bennett, M.R. & Legrand, L. (1992) Biomechanical analysis of jumping in *Anolis carolinensis* (Reptilia; Iguanidae). *Copeia*, 1992, 492–504.

Birn-Jeffery, A.V. & Higham, T.E. (2014) Geckos significantly alter foot orientation to facilitate adhesion during downhill locomotion. *Biology Letters*, 10(10), 20140456.

Borsuk-Białynicka, M. (2018) Diversity of diapsid fifth metatarsals from the lower Triassic karst deposits of Czatkowice, southern Poland—functional and phylogenetic implications. *Acta Palaeontologica Polonica*, 63, 417–434.

Brinkman, D. (1980) Structural correlates of tarsal and metatarsal functioning in *Iguana* (Lacertilia: Iguanidae) and other lizards. *Canadian Journal of Zoology*, 58, 277–289.

Buettell, K. & Losos, J.B. (1999) Ecological morphology of Caribbean anoles. *Herpetological Monographs*, 13, 1–28.

Clark, A.D. & O'Connor, J.K. (2021) Exploring the ecomorphology of two cretaceous enantiornithines with unique pedal morphology. *Frontiers in Ecology and Evolution*, 9, 654156. Available from: https://doi.org/10.3389/fevo.2021.54156

Dang, N.-X., Wang, J.-S., Liang, J., Jiang, D.C., Liu, J., Wang, L. et al. (2018) The specialisation of the third metacarpal and hand in arboreal frogs: adaptation for arboreal habitat? *Acta Zoologica*, 99, 115–125.

de Queiroz, K. (2022) The correct name for the taxon ranked as a family containing the gnus *Anolis* under rank-based nomenclature and the author of the name *Anolis loysiana*. *Herpetological Review*, 53, 418–420.

DiPaolo, E.C.C. & Kolbe, J. (2023) Blowing in the wind: experimental assessment of clinging performance and behaviour in *Anolis* lizards during hurricane-force winds. *Functional Ecology*, 37, 639–647.

Donihue, C.M., Herrel, A., Fabre, A.-C., Kamath, A., Genova, A.J., Schoener, T.W. et al. (2018) Hurricane-induced selection on the morphology of an island lizard. *Nature*, 560, 88–91.

Evans, S.E. (2003) At the feet of the dinosaurs: the early history and radiation of lizards. *Biological Reviews*, 78, 513–551.

Foster, K.L. & Higham, T.E. (2012) How fore- and hindlimb function changes with incline and perch diameter in the green anole (*Anolis carolinensis*). *Journal of Experimental Biology*, 215, 2288–2300.

Gamble, T., Greenbaum, E., Jackman, T.R., Russell, A.P. & Bauer, A.M. (2012) Repeated origin and loss of adhesive toepads in geckos. *PLoS One*, 7, e39429.

Garner, A.M., Wilson, M.C., Russell, A.P., Dhinojwala, A. & Niewiarowski, P.H. (2019) Going out on a limb: how investigation of the anoline adhesive system can enhance our understanding of fibrillar adhesion. *Integrative and Comparative Biology*, 59, 61–69.

Garner, A.M., Wilson, M.C., Wright, C., Russell, A.P., Niewiarowski, P.H. & Dhinojwala, A. (2021) The same but different: setal arrays of anoles and geckos indicate alternative approaches to achieving similar adhesive effectiveness. *Journal of Anatomy*, 238, 1143–1155.

Gillis, G.B., Bonvini, L.A. & Irschick, D.J. (2009) Losing stability: tail loss and jumping in the arboreal lizard *Anolis carolinensis*. *Journal of Experimental Biology*, 212, 604–609.

Goodrich, E.S. (1916) On the classification of the Reptilia. *Proceedings of the Royal Society of London Series B*, 89, 261–276.

Griffing, A.H., Gamble, T., Cohn, M.J. & Sanger, T.J. (2022) Convergent developmental patterns underlie the repeated evolution of toe pads among lizards. *Biological Journal of the Linnean Society*, 135, 518–532.

Hagey, T.J., Harte, S., Vickers, M., Harmon, L.J. & Schwarzkopf, L. (2017) Thee's more than one way to climb a tree: limb length and microhabitat use in lizards with toe pads. *PLoS One*, 12(9), e0184641. Available from: https://doi.org/10.1371/journal.pone.0184641

Hagey, T.J., Uyeda, J.C., Crandell, K.E., Cheney, J.A., Autumn, K. & Harmon, L.J. (2017) Tempo and mode of performance evolution across multiple independent origins of adhesive toepads in lizards. *Evolution*, 71, 2344–2358.

Higham, T.E., Davenport, M.S. & Jayne, B.C. (2001) Maneuvering in an arboreal habitat: the effects of turning angle on the locomotion of three sympatric ecomorphs of *Anolis* lizards. *Journal of Experimental Biology*, 204, 4141–4155.

Higham, T.E., Gamble, T. & Russell, A.P. (2017) On the origin of frictional adhesion in geckos: small morphological changes lead to a major biomechanical transition in the genus *Gonatodes*. *Biological Journal of the Linnean Society*, 120, 503–517.

Higham, T.E. & Russell, A.P. (2025) Geckos running with dynamic adhesion: towards integration of ecology, energetics and biomechanics. *Journal of Experimental Biology*. 228 (Suppl 1): JEB247980

Higham, T.E., Zhuang, M. & Russell, A.P. (2021) Ankle structure of the Tokay gecko (*Gekko gecko*) and its role in the deployment of the subdigital adhesive system. *Journal of Anatomy*, 239, 1503–1515.

Irschick, D.J., Austin, C.C., Petren, K., Fisher, R.N., Losos, J.B. & Ellers, O. (1996) A comparative analysis of clinging ability among pad-bearing lizards. *Biological Journal of the Linnean Society*, 59, 21–35.

Irschick, D.J., Carlisle, E., Elstrott, J., Ramos, M., Buckley, C., Vanhooydonck, B. et al. (2005) A comparison of habitat use, morphology, clinging performance and escape behaviour among two divergent green anole lizard (*Anolis carolinensis*) populations. *Biological Journal of the Linnean Society*, 85, 223–234.

Irschick, D.J. & Losos, J.B. (1998) A comparative analysis of the ecological significance of maximal locomotor performance in Caribbean *Anolis* lizards. *Evolution*, 52, 219–226.

Losos, J.B. (2009) *Lizards in an evolutionary tree: ecology and adaptive radiation of anoles*. Berkeley, CA: University of California Press.

Losos, J.B. & Irschick, D.J. (1996) The effect of perch diameter on escape behavior of *Anolis* lizards: laboratory predictions and field tests. *Animal Behaviour*, 51, 593–602.

Losos, J.B. & Sinervo, B. (1989) The effects of morphology and perch diameter on sprint performance of *Anolis* lizards. *Journal of Experimental Biology*, 145, 23–30.

Maderson, P.F.A. (1970) Lizard glands and lizard hands: models for evolutionary study. *Forma et Functio*, 3, 179–204.

Mattingly, W.B. & Jayne, B.C. (2004) Resource use in arboreal habitats: structure affects locomotion of four ecomorphs of *Anolis* lizards. *Ecology*, 85, 1111–1124.

Miller, A.H. & Stroud, J.T. (2022) Novel tests of the key innovation hypothesis: adhesive toepads in arboreal lizards. *Systematic Biology*, 71, 139–152.

Moermond, T.C. (1979) Habitat constraints on the behavior, morphology and community structure of *Anolis* lizards. *Ecology*, 60, 152–164.

Pounds, J.A. (1988) Ecomorphology, locomotion, and microhabitat structure: patterns in a tropical mainland *Anolis* community. *Ecological Monographs*, 58, 299–320.

Rand, A.S. (1967) Ecology and social organization in the iguanid lizard *Anolis lineatopus*. *Proceedings of the United States National Museum*, 122(3595), 1–79.

Regnault, S., Jones, M.E.H., Pitsillides, A.A. & Hutchinson, J.R. (2016) Anatomy, morphology and evolution of the patella in squamate lizards and tuatara (*Sphenodon punctatus*). *Journal of Anatomy*, 228, 864–876.

Rewcastle, S.C. (1980) Form and function in lacertilian knee and mesotarsal joints: a contribution to the analysis of sprawling locomotion. *Journal of Zoology*, 191, 147–170.

Rewcastle, S.C. (1981) Stance and gait in tetrapods: an evolutionary scenario. *Symposia of the Zoological Society of London*, 48, 239–267.

Rewcastle, S.C. (1983) Fundamental adaptations in the lacertilian hindlimb: a partial analysis of the sprawling limb posture and gait. *Copeia*, 1983, 467–487.

Rivero-Blanco, C. (1976) Osteology of the lizard *Gonatodes humeralis* (Guichenot) and other representative species of the genus. MSc thesis, College Station, TX: Texas Agricultural and Mechanical University, p xxii + 122.

Robinson, P.L. (1975) The functions of the hooked fifth metatarsal in lepidosaurian reptiles. In: Lehman, M.J.-P. (Ed.) *Problèmes Actuelles de Paleontologie—Evolution des Vertebrès*, Vol. 218. Paris: Colloques International du C.N.R.S, pp. 461–483.

Rothier, P.S., Brandt, R. & Kohlsdorf, T. (2017) Ecological associations of autopodial osteology in neotropical geckos. *Journal of Morphology*, 278, 290–299.

Ruibal, R. & Ernst, V. (1965) The structure of the digital setae of lizards. *Journal of Morphology*, 117, 271–293.

Russell, A.P. (1975) A contribution to the functional analysis of the foot of the Tokay, *Gekko gecko* (Reptilia: Gekkonidae). *Journal of Zoology*, 176, 437–476.

Russell, A.P. (1993) The aponeuroses of the lacertilian ankle. *Journal of Morphology*, 218, 65–84.

Russell, A.P. (2002) Integrative functional morphology of the gekkotan adhesive system. *Integrative and Comparative Biology*, 42, 1154–1163.

Russell, A.P., Baskerville, J., Gamble, T. & Higham, T.E. (2015) The origin of digit form in *Gonatodes* (Gekkota: Sphaerodactylidae) and its bearing on the transition from frictional to adhesive contact in gekkotans. *Journal of Morphology*, 276, 1311–1332.

Russell, A.P. & Bauer, A.M. (2008) The appendicular locomotor apparatus of *Sphenodon* and normal-limbed squamates. In: Gans, C., Gaunt, A.S. & Adler, K. (Eds.) *Biology of the Reptilia*, Vol. 21. Ithaca, NY: Society for the Study of Amphibians and Reptiles, pp. 1–466.

Russell, A.P., Bauer, A.M. & Laroiya, R. (1997) Morphological correlates of the secondarily symmetrical pes of gekkotan lizards. *Journal of Zoology*, 241, 767–790.

Russell, A.P. & Bels, V. (2001) Digital hyperextension in *Anolis sagrei*. *Herpetologica*, 57, 58–65.

Russell, A.P. & Gamble, T. (2019) Evolution of the gekkotan adhesive system: does digit anatomy point to one or more origins? *Integrative and Comparative Biology*, 59, 131–147.

Russell, A.P. & Garner, A.M. (2023) Solutions to a sticky problem: convergence of the adhesive systems of geckos and anoles (Reptilia: Squamata). In: Bels, V.L. & Russell, A.P. (Eds.) *Convergent evolution. Fascinating life sciences*. Chamonix, Switzerland: Springer, pp. 221–255.

Russell, A.P. & Higham, T.E. (2009) A new angle on clinging in geckos: incline, not substrate, triggers the deployment of the adhesive system. *Proceedings of the Royal Society B*, 276, 3705–3709. Available from: https://doi.org/10.1098/rspb.2009.0946

Russell, A.P. & Oetelaar, G.S. (2016) Limb and digit orientation during vertical clinging in Bibron's gecko, *Chondrodactylus bibronii* (A. Smith, 1846) and its bearing on the adhesive capabilities of geckos. *Acta Zoologica*, 97, 345–360.

Russell, A.P. & Rewcastle, S.C. (1979) Digital reduction in *Sitana* (Reptilia: Agamidae) and the dual roles of the fifth metatarsal in lizards. *Canadian Journal of Zoology*, 57, 1129–1135.

Schoener, T.W. & Schoener, A. (1971) Structural habitats of West Indian *Anolis* lizards. I. Lowland Jamaica. *Breviora*, 368, 1–53.

Simoes, T.R., Caldwell, M.W., Nydam, R.L. & Jiménez-Huidobro, P. (2016) Osteology, phylogeny and functional morphology of two Jurassic lizard species and the early evolution of scansoriality in geckos. *Zoological Journal of the Linnean Society*, 180, 216–241.

Song, Y., Dai, Z., Wang, Z. & Full, R.J. (2020) Role of multiple adjustable toes in distributed control shown by the sideways wall-running in geckos. *Proceedings of the Royal Society B: Biological Sciences*, 287, 20200123. Available from: https://doi.org/10.1098/rspb.2020.0123

Toro, E., Herrel, A. & Irschick, D. (2004) The evolution of jumping performance in Caribbean *Anolis* lizards: solutions to biomechanical tradeoffs. *The American Naturalist*, 163, 844–856.

Toro, E., Herrel, A., Vanhooydonck, B. & Irschick, D.J. (2003) A biomechanical analysis of intra- and interspecific scaling of jumping and morphology in Caribbean *Anolis* lizards. *Journal of Experimental Biology*, 206, 2641–2652.

Wainwright, P.C., Alfaro, M.E., Bolnick, D.I. & Hulsey, C.D. (2005) Many-to-one mapping of form to function: a general principle in organismic design? *Integrative and Comparative Biology*, 45, 256–262.

Wright, A.N., Kennedy-Gold, S.R., Naylor, E.R., Screen, R.M., Piantoni, C. & Higham, T.E. (2021) Clinging performance on natural substrates predicts habitat use in anoles and geckos. *Functional Ecology*, 35, 2472–2482.

Zaaf, A., Van Damme, R., Herrel, A. & Aerts, P. (2001) Limb joint kinematics during vertical climbing and level running in a specialist climber: *Gekko gecko* Linneus (sic), 1758 (Lacertilia: Gekkonidae). *Belgian Journal of Zoology*, 131, 173–182.

Zhuang, M.V. & Higham, T.E. (2016) Arboreal day geckos (*Phelsuma madagascariensis*) differentially modulate fore- and hindlimb kinematics in response to changes in habitat structure. *PLoS One*, 11(5), e0153520. Available from: https://doi.org/10.1371/journal.pone.0153520

Zhuang, M.V., Russell, A.P. & Higham, T.E. (2019) Evolution of pedal digit orientation and morphology in relation to acquisition and secondary loss of the adhesive system in geckos. *Journal of Morphology*, 280, 1582–1599.

How to cite this article: Russell, A.P., McGregor, L.D. & Higham, T.E. (2025) Osteology and arthrology of the ankle and tarsometatarsus of anoles (Iguania: Anolidae): not convergent with geckos but divergent from the ancestral iguanian condition. *Journal of Anatomy*, 00, 1–24. Available from: https://doi.org/10.1111/joa.70007